SLAC – PUB – 4253
March 1987
T/E

PHENOMENOLOGY OF HEAVY QUARK SYSTEMS*

FREDERICK J. GILMAN

Stanford Linear Accelerator Center

Stanford University, Stanford, California, 94305

Presented at the SLAC Summer Institute on Particle Physics,
Stanford, CA., July 28- August 8, 1986

* Work supported by the Department of Energy, contract DE – AC03 – 76SF00515.

1. Heavy Quark Spectroscopy

Introduction

The spectroscopy of heavy quark systems is the showcase of our understanding of hadron physics. It is sometimes even advertised as the "hydrogen atom of strong interactions".

We do indeed have a fundamental gauge theory of the strong interactions in Quantum Chromodynamics (QCD). This theory in principle explains the vast body of data that has been accumulated over the past dozen years.[1] However, as we will soon see, the connection between the fundamental theory and experimental observables is not (yet) as it is for the electroweak gauge theory, $SU(2) \times U(1)$. The situation we confront is essentially non-perturbative, and the underlying gauge theory is one-step-removed from detailed numerical confrontation with experiment.

What we have at present to accompany the data is more like a phenomenology, inspired or backed-up by QCD. At times it gives us an asymptotic form. At other times it gives an expression for the general structure of some quantity, with free parameters or hadronic matrix elements contained within it. While these latter are determined by QCD in principle, for the moment they are often only approximately calculable (at best). So we take a peek at the data and 'adjust' the parameters, thereby learning something about the nature of the solution of QCD. Then we predict additional quantities and iterate the whole process again.

This is then a place where theory and experiment intertwine; basic theory, models inspired by theory, and experiment meet and influence one another. It is

quite different from the situation in the electroweak theory where there is a well-defined and clean set of perturbative predictions to compare with experiment. In one sense this is frustrating, as one would like clean and decisive tests of the underlying theory. In another sense, this is what makes it exciting and makes the subject still worth pursuing: the interplay between theory and experiment is interesting in itself, and we often learn things which are applicable either as techniques or as results in other areas as well.

In fact, progress has been made and continues to be made.[2] Eventually, one has every reason to believe that we will be able to calculate the "potential" from first principles, presumably using lattice techniques. Everything then will be predicted starting from the QCD Lagrangian. We have come a long way in this direction already,[3] and perhaps in the Summer Institute of a few(?) years hence we may well no longer need a talk on this subject.

The Spin Independent Potential

Let's start with the nonrelativistic, spin independent potential. Even the use of the word potential is a bit loose for we are starting with a strong interaction bound state problem and extracting from it an effective two-body, non-relativistic potential. The problem at hand is intrinsically a relativistic field-theoretic one in which the $q\bar{q}$ sector, for example, is coupled to what happens in the $qq\bar{q}\bar{q}$, $q\bar{q}$ + gluon, etc. sectors as well. Some justification for the success of the "naive," non-relativistic approach have recently been given,[4] but simultaneously questions have been raised as to the effect of what is being neglected, and how it changes the relationship between parameters in the underlying theory and the effective potential.[5] There is even a whole, well-developed approach to understanding

some of the same body of data through QCD sum rules.[6]

With these questions in mind, we shall proceed to think in terms of a two-body potential obtained by expanding in powers of v^2/c^2. Indeed, such an expansion does make some sense, for the smallness of v^2/c^2 in a system composed of a heavy quark and heavy antiquark encourages us to think in terms of a non-relativistic potential with spin-dependent terms which arise first in order v^2/c^2 and give rise to splittings which are smaller than those between levels of the spin independent potential. In the cases at hand v^2/c^2 is ~ 0.4 for the low-lying charmonium states and $\lesssim 0.1$ for the low-lying bottomonium states. Still, when we go to compare with the calculated energy levels with experiment we need to bear in mind that predictions from alternate potentials that differ by 10 or 20 MeV are not necessarily significant in favoring one potential over another. We may in any case be making (especially for charmonium) approximations to the exact theory in "deriving" a non-relativistic potential which render the resulting model incapable of discriminating differences at this level.

We have good theoretical guidance in two opposite regimes. At short distances, or equivalently large momentum scales, there is the property of asymptotic freedom. The running coupling becomes smaller as we decrease the distance scale at which we work, and the effective potential approaches the lowest order one gluon exchange result,

$$V(r) \to -\frac{4}{3}\frac{\alpha_s}{r} \tag{1}$$

as $r \to 0$.

Note the additional factor of $\frac{4}{3}$ compared to the usual Coulomb interaction; this arises from color. Its derivation was discussed in the Summer Institute of

10 years ago.[7] It is so pervasive that it is worth a short derivation, so here it is again. We want the additional factor due to color. It arises from a normalized color singlet quark-antiquark wave function, $\delta_{ij}/\sqrt{3}$ in the initial and final state, a color SU(3) matrix $\lambda^a_{ij}/2$ at each quark-gluon vertex, and a color sum over the (eight) gluons, δ^{ab}, in the gluon propagator. The sum over indices gives a trace:

$$\sum_{a,b=1}^{8} \sum_{i,j,k,l=1}^{3} \frac{\delta_{il}}{\sqrt{3}} \frac{\lambda^a_{ij}}{2} \frac{\delta_{jk}}{\sqrt{3}} \frac{\lambda^b_{kl}}{2} \delta^{ab} = \frac{1}{3} \sum_{a=1}^{8} Tr\left[\frac{\lambda^a}{2}\frac{\lambda^a}{2}\right] = \frac{1}{3}(8)\frac{1}{2} = \frac{4}{3}. \quad (2)$$

The trace of $\frac{\lambda^a}{2}\frac{\lambda^a}{2}$ is just $\frac{1}{2}$, as befits the generators of a Lie algebra (or, as may be checked for the case of the λ matrices of $SU(3)$ directly); thus the ubiquitous factor of 4/3.

That's one regime. The second regime where we have very solid theoretical input is at the other extreme, as $r \to \infty$, and we have confinement of the quarks. From relatively general theoretical arguments we know that the potential behaves as a linear function of the distance:

$$V(r) \to kr. \quad (3)$$

There is a corresponding physical picture of a "color-electric flux tube" joining the quarks. As you pull the quarks apart, the flux tube is increased in length, at the cost of an increase in energy per unit length given by the constant k. The value of k is about 0.2 GeV^2.

Given those two regimes we might hope to construct the full potential. The simplest possibility is to simply add together terms with the correct functional de-

pendence in the two asymptotic regimes. This is basically the Cornell potential,[8]

$$V(r) = \frac{-0.48}{r} + \frac{r}{(2.34\ \mathrm{GeV}^{-1})^2}, \tag{4}$$

with the two coefficients having been adjusted to fit the charmonium spectrum, although the model does a quite adequate job in describing bottomonium as well.

In the late 70's Richardson combined the two behaviors in one form.[9] Here is his potential in configuration space,

$$V(r) = \frac{8\pi}{33 - 2n_f}\,\Lambda\left(\Lambda r - \frac{f(\Lambda r)}{\Lambda r}\right), \tag{5}$$

with

$$f(t) = 1 - 4\int_1^\infty \frac{dq}{q}\,\frac{e^{-qt}}{\ell n^2(q^2-1) + \pi^2}, \tag{6}$$

where it looks like two terms. What's going on is more transparent in momentum space where it can be written as one term:

$$\widetilde{V}(q^2) = -\frac{4}{3}\,\frac{12\pi}{33 - 2n_f}\,\frac{1}{q^2 \ell n(1 + q^2/\Lambda^2)}. \tag{7}$$

As q^2 goes to infinity, this expression becomes precisely $\frac{4}{3}\alpha_s/q^2$, as required from one gluon exchange. In the other limit of $q^2 \to 0$, one obtains something proportional to $1/q^4$. This may be an unfamiliar behavior in momentum space, but if you Fourier transform back to configuration space, this is just a potential which is linear in r. It is by no means guaranteed that you will get the "right" coefficient to fit the data. Richardson, along with others[10] who proposed modified versions of this potential, showed that you do in fact get a very reasonable, even excellent, description of the data, especially for bottomonium.

Finally, Martin has proposed the potential[11]

$$V(r) = (5.82 \text{ GeV}) \left(\frac{r}{1 \text{ GeV}^{-1}}\right)^{0.104} . \tag{8}$$

This potential, with the absurd power of 0.104, lacks fundamental motivation (as Martin knew very well). We will use it as a kind of straw man, for it also does quite a credible job of fitting the charmonium and bottomonium data. But why?

The reason can be seen in Figure 1. Here you can see the various potentials for comparison purposes. In particular, aside from being displaced vertically from one another a little bit (which you are free to remove by adjusting the quark mass), they all have about the same behavior between 0.1 and 1 fermi. This can be seen even better looking at the inset, where r is given on a logarithmic scale and the potentials have been shifted slightly relative to one another vertically, as discussed above. Also shown are the mean radii of the psi, upsilon, etc. These are all between 0.1 and 1 fermi, and that's why the different potentials all can fit the data; the wave functions for these states mostly (but not entirely) live in this region where the potentials coincide.

Thus, where our theoretical insight is best and tells us something very well-defined for the behavior of the spin independent potential, it is mostly irrelevant to the present data. Conversely, the experiments up to now mostly tell us about a region where theory does not have much to say about the spin independent potential. In fact, one can invert the data to obtain a potential[12] which describes what happens from 0.1 to 1 fermi. Within errors, it coincides with what we have just seen in Figure 1.

Even without a particular potential and detailed calculation, we can get a good qualitative idea of what the spectrum of states will look like. In Figure 2a

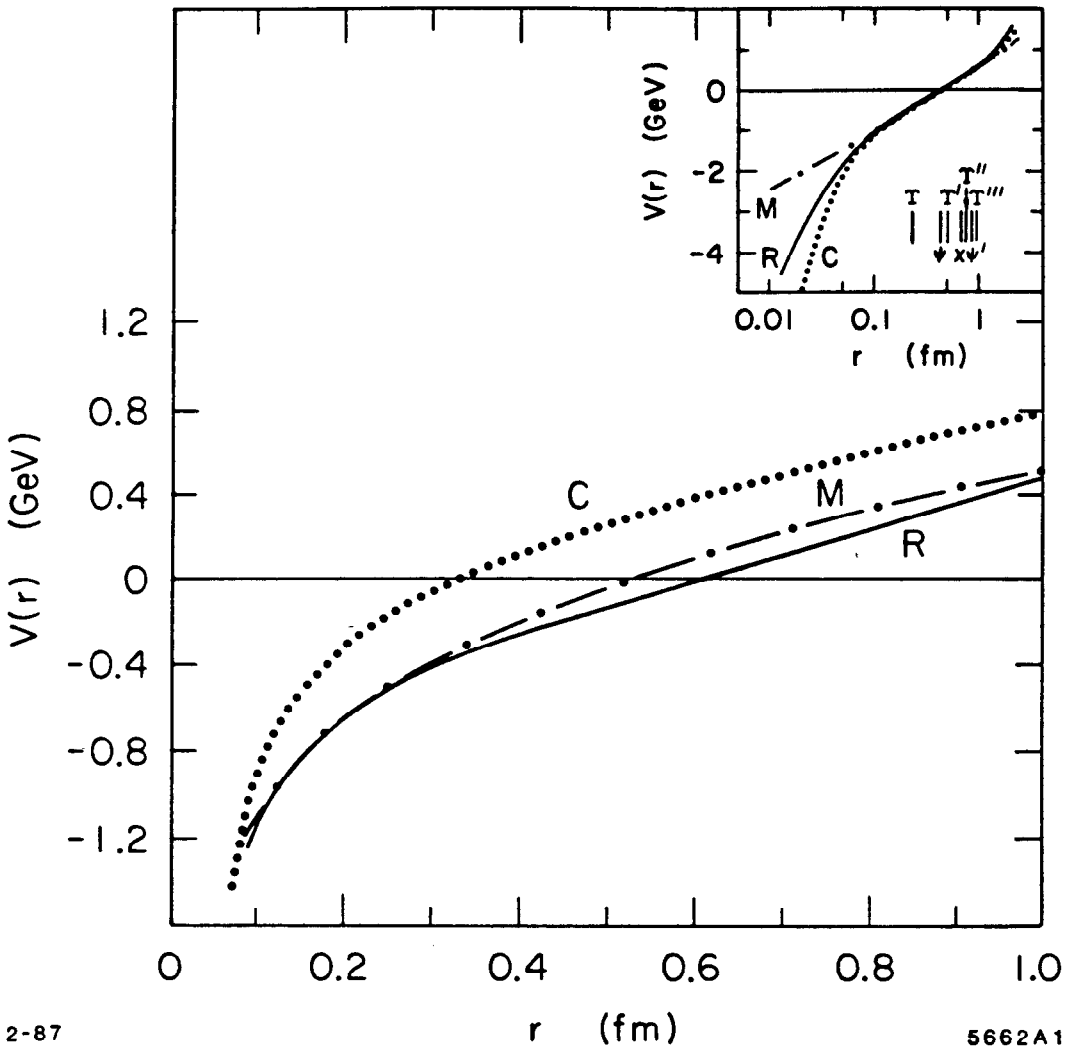

Fig. 1. Comparison of the shape of the Cornell[8] (dotted curve), Richardson[9,10] (solid curve), and Martin[11] (dash-dot curve) potentials. The inset shows the same comparison with the potentials displaced slightly on the vertical scale and a logarithmic horizontal scale, along with the mean radii of some charmonium and bottomonium states.

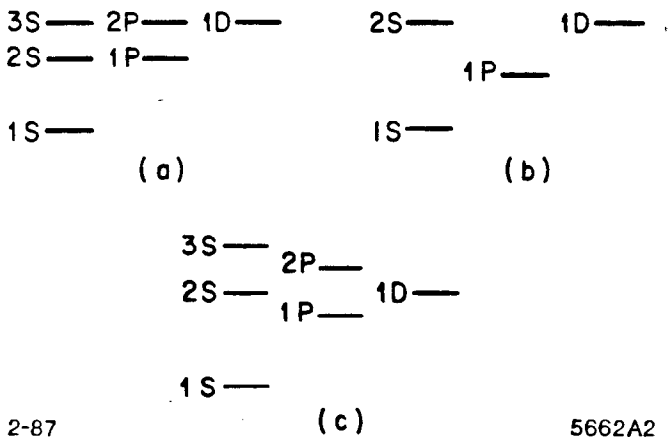

Fig. 2. The spectrum of energy levels in the case of the Coulomb potential (a), the three dimensional harmonic oscillator (2b), and a hybrid of the two (c).

is the familiar spectrum due to a Coulomb potential, which is what we have at short distances. The ground state with $\ell = 0$ is labelled 1S; its radial excitation (labelled 2S) is degenerate in the case of a Coulomb potential with the first set of $\ell = 1$ states (labelled 1P), and so on. As an example of a confining potential which we want at large distance, Figure 2b shows the levels of a three dimensional harmonic oscillator, which is more familiar than a linear potential and turns out also to be a special "boundary" case from the point of view of the ordering of levels. What will happen when we combine the two? For the energy levels we will naturally get something in between Figures 2a and 2b. This is shown in Figure 2c. The ordering, starting at the bottom, is 1S, 1P (between the 1S and 2S as for the harmonic oscillator, but closer to the 2S, as it would be degenerate with it for the Coulomb potential), 2S, 1D (above 2S as for Coulomb, but close to it, as it would be degenerate for the harmonic oscillator), etc. You can therefore get a qualitative understanding of the spectrum from quite general considerations.

There is a theorem[13] which is quite useful in this regard and puts the qualitative ordering discussed above on a rigorous footing. It states that if $\bigtriangledown^2 V(r) > 0$ for all r, something which is true for all suggested potentials, then $E_{nS} > E_{(n-1)P}$. Related theorems are provable for the ordering of levels with other angular momenta.[14]

Each of the potentials discussed above can give a quantitative understanding of the levels of charmonium and bottomonium to 30 MeV or better. Even the statement that one flavor independent potential can fit both systems is nontrivial. The agreement between theory and experiment, which is shown in Schindler's lectures,[1] I regard as quite spectacular. It includes not just energy levels, but wave functions at the origin for the nS states as well. Where there is a disagree-

ment, it is difficult to know whether to blame it on the potential or on corrections due to relativistic or other effects which have been left out.

When and how will we be able to distinguish between potentials? The answer appears to be that toponium will provide the crucial system. In Figure 3 is shown the spectrum of toponium[15] corresponding to m_t in the range of 40 to 50 GeV. There are 10 or more nS states below open top threshold; near that threshold there is one state per 100 MeV.

More important for the physics at hand, aspects of the spectrum of states and of the wave functions at the origin are now sensitive to the behavior of the potential at short distances. The values of the wave function at the origin are shown in Figure 4, with that for the ground state corresponding to a width into electron-positron pairs, which is proportional to the square of the wave function at the origin, of about 9 keV (from the one photon intermediate state alone). This is larger than one would expect from a naive extrapolation from the psi and the upsilon by about a factor of two. We are beginning to see the effect of the 1/r term in the potential pulling in the wave function. Higher levels are affected less, as seen in Figure 4, for on average they live at larger distances.

The same physical effect is shown in Table I, with the t quark mass assumed to be 50 GeV. Notice in particular how much the energy of the 1S level is pulled down by the Cornell potential (3 GeV below 2 m_t). This is to be compared with 1.7 GeV for the Richardson and 1.4 GeV for the Martin potentials. Correspondingly the radius of the 1S state is much smaller for the Cornell potential and the 2S to 1S difference much bigger. Even more dramatic is the comparison of the wave function at the origin for the 1S state, where the Cornell result is about 3 times that for Richardson and 9 times that for Martin. Remember, the predicted

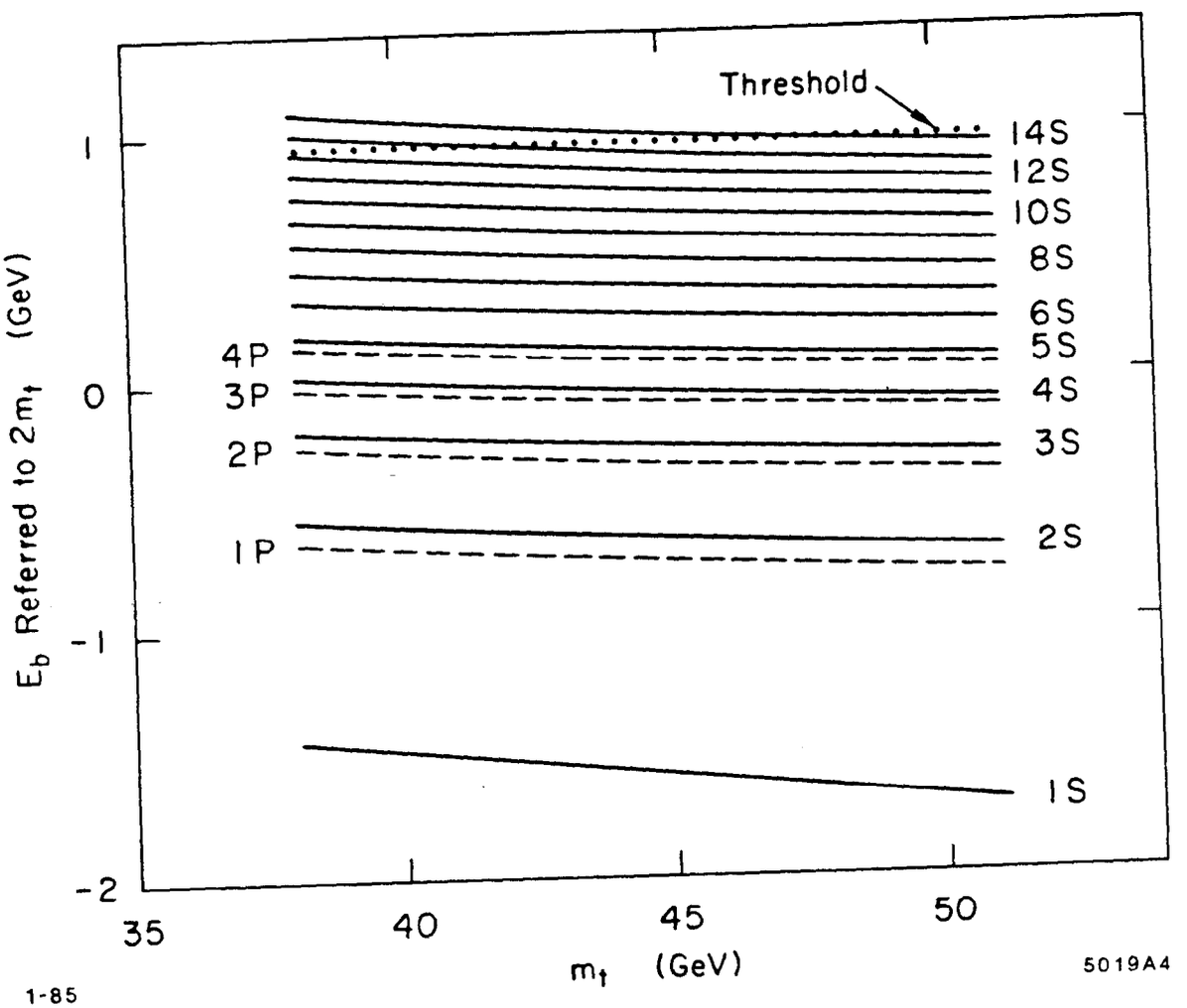

Fig. 3. The spectrum of nS states of toponium obtained[15] from the Richardson potential with m_t in the range of 40 to 50 GeV.

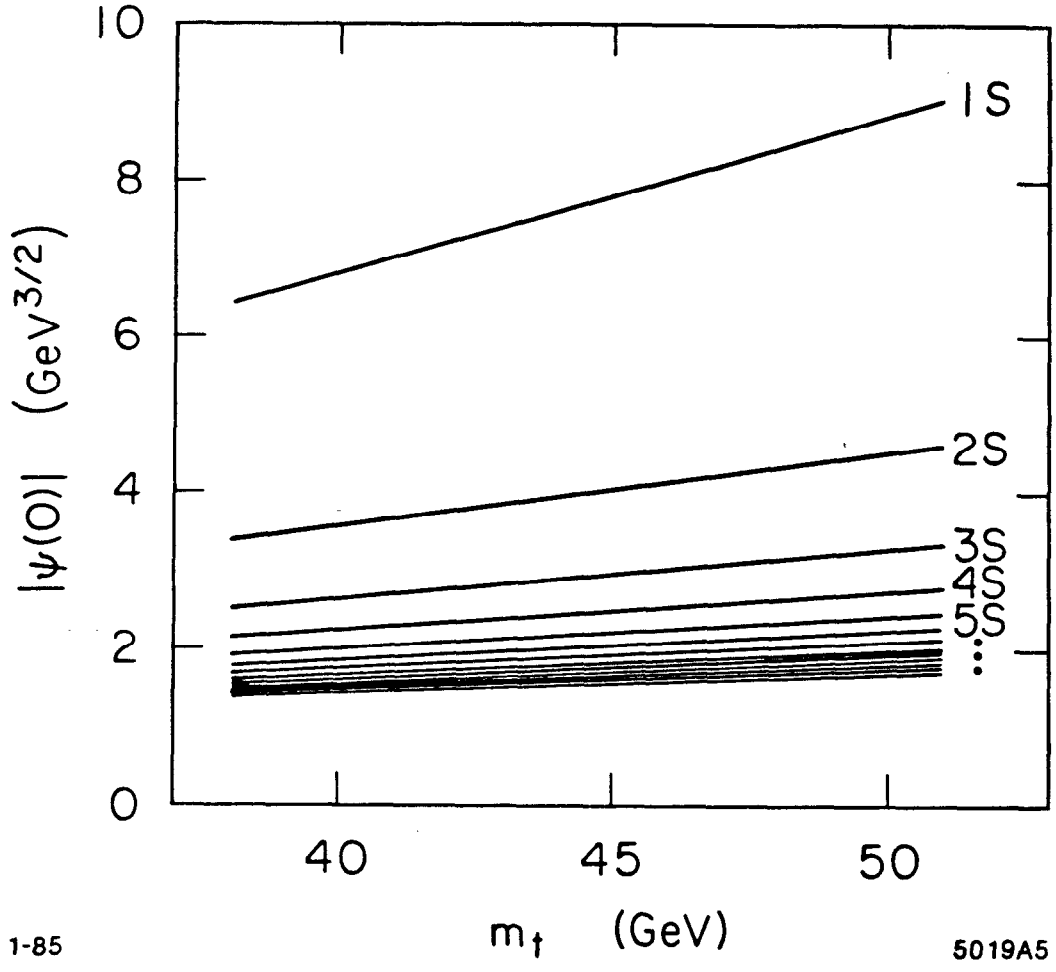

Fig. 4. The value of the wave function at the origin for toponium nS states obtained[15] with the Richardson potential and m_t in the range of 40 to 50 GeV.

electron-positron width goes like these numbers squared!

Potential	E_{1S} (GeV)	$< r_{1S} >$ (fermi)	$E_{2S} - E_{1S}$ (GeV)	$\Psi(0)_{1S}$ ($GeV^{3/2}$)
"Cornell"	97.1	0.028	2.2	23.3
"Richardson"	98.3	0.048	1.0	8.5
"Martin"	98.6	0.084	0.5	2.7

Table 1. Characteristics of Toponium States for Various Potentials

Before leaving this subject, we should note that this same property makes toponium a fairly sensitive place to look for extra short range forces. A good example is the presence of an extra term in the potential due to neutral Higgs exchange with enhanced couplings.[16] This changes both the wave functions and the ordering of the energy levels in a characteristic fashion, and allows it to be distinguished from a simple change in the strength of the 1/r piece of the strong interaction potential.

The Spin Dependent Potential

Now we turn to the spin dependent potential. In its full glory it has the form:

$$
\begin{aligned}
V_{SD}(r) = & \left(\frac{\vec{S}_1 \cdot \vec{L}}{2m_1^2} + \frac{\vec{S}_2 \cdot \vec{L}}{2m_2^2} \right) \left(\frac{dV(r)}{rdr} + 2\frac{dV_1(r)}{rdr} \right) \\
& + \frac{(\vec{S}_1 + \vec{S}_2) \cdot \vec{L}}{m_1 m_2} \frac{dV_2(r)}{rdr} \\
& + \frac{1}{6m_1 m_2} \left(6\vec{S}_1 \cdot \hat{r} \vec{S}_2 \cdot \hat{r} - 2\vec{S}_1 \cdot \vec{S}_2 \right) V_3(r) \\
& + \frac{2}{3m_1 m_2} \vec{S}_1 \cdot \vec{S}_2 \, V_4(r)
\end{aligned}
\tag{9}
$$

as given by Eichten and Feinberg[17] and discussed at previous Summer Institutes by Eichten[18] and by Peskin.[19] The term V(r) is the spin independent potential we discussed previously. The other terms involving V_1, V_2, V_3, and V_4 are not necessarily simply related to V(r). As can be seen particularly clearly in Michael Peskin's lectures,[19] these extra terms originate in expectation values of color electric and magnet fields which are different than those that enter in the spin independent potential; they are new objects.

Although the situation is more complicated than one might have hoped, at least initially it was possible to entertain the idea that all the new spin dependent terms are of short range. This hope was dashed when it was shown that[20]

$$
V(r) + V_1(r) = V_2(r). \tag{10}
$$

Since V has a long range confining part, so must either V_1 or V_2.

Let us use Eq. (10) to eliminate V_1 from the spin dependent potential. It now reads:

$$V_{SD}(r) = \left(\frac{\vec{S}_1 \cdot \vec{L}}{2m_1^2} + \frac{\vec{S}_2 \cdot \vec{L}}{2m_2^2}\right) \left(\frac{-dV(r)}{rdr} + 2\frac{dV_2(r)}{rdr}\right)$$
$$+ \frac{(\vec{S}_1 + \vec{S}_2) \cdot \vec{L}}{m_1 m_2} \frac{dV_2(r)}{rdr}$$
$$+ \frac{1}{6m_1 m_2}\left(6\vec{S}_1 \cdot \hat{r}\vec{S}_2 \cdot \hat{r} - 2\vec{S}_1 \cdot \vec{S}_2\right) V_3(r) \qquad (11)$$
$$+ \frac{2}{3m_1 m_2}\vec{S}_1 \cdot \vec{S}_2 \, V_4(r).$$

Could it now be that the remaining new potentials V_2, V_3, and V_4 are short range?

Not only is there no information to contradict this possibility, but it is supported by the results of recent lattice gauge theory calculations,[21,22] the results of some of which[22] are shown in Figures 5, 6, 7, and 8. We see that V_1 (which we have eliminated from Eq. (11)) is not short range, but V_2 looks completely different; it is very short range, and similarly for V_3 and V_4. All of this is done on a $16^3 \times 32$ lattice. It should be regarded as a qualitative result, but an important step toward the more quantitative results we can expect in the future.

Let us now go back to the spin dependent potential in the equal mass case relevant to quarkonium. We rewrite it a little bit, combining the first two terms:

$$V_{SD}(r) = \frac{\vec{S} \cdot \vec{L}}{2m^2} \left(\frac{-dV(r)}{rdr} + 4\frac{dV_2(r)}{rdr}\right)$$
$$+ \frac{1}{12m^2}\left(6\vec{S} \cdot \hat{r}\vec{S} \cdot \hat{r} - 2\vec{S} \cdot \vec{S}\right) V_3(r) \qquad (12)$$
$$+ \frac{1}{6m^2}\left(2\,\vec{S} \cdot \vec{S} - 3\right) V_4(r).$$

Now, to get a simple physical picture of what is happening, let us forget for a

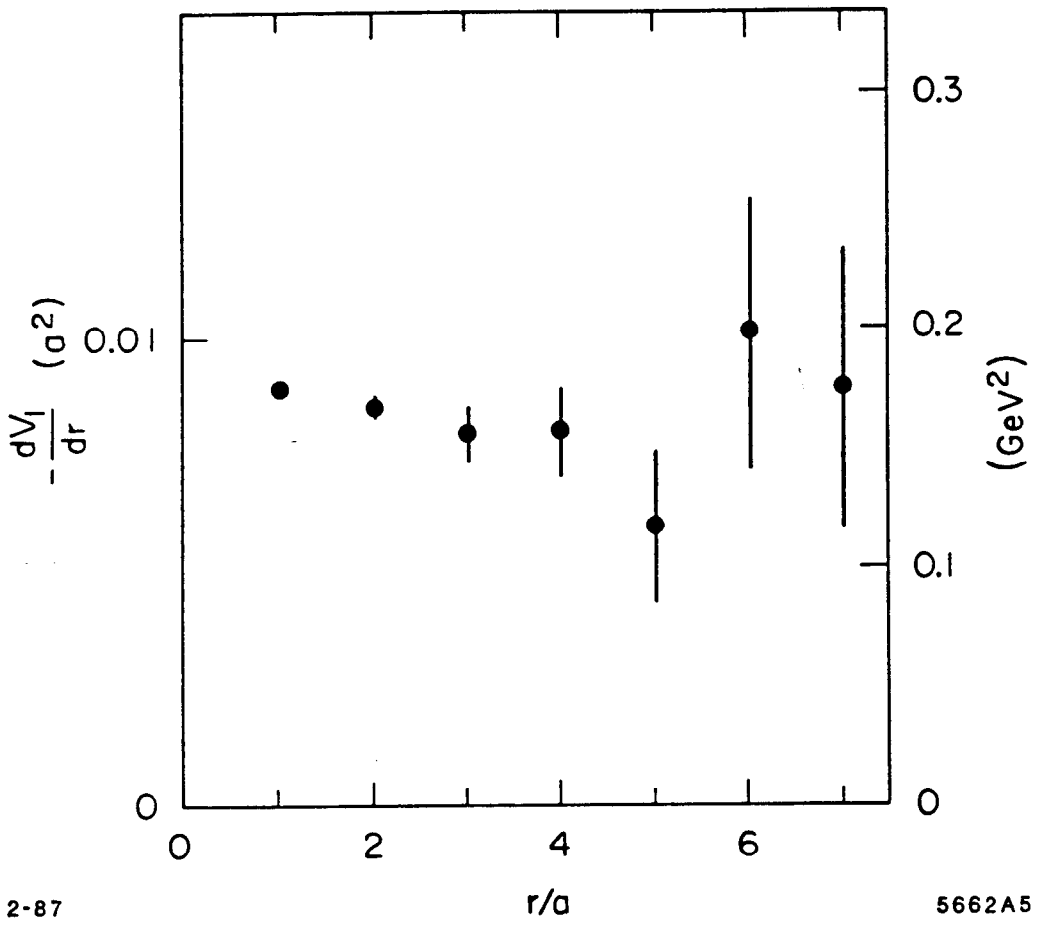

Fig. 5. Results of a lattice Monte Carlo calculation[22] of the spin-dependent potential $-dV_1/dr$ as a function of radial distance in units of the lattice spacing, a.

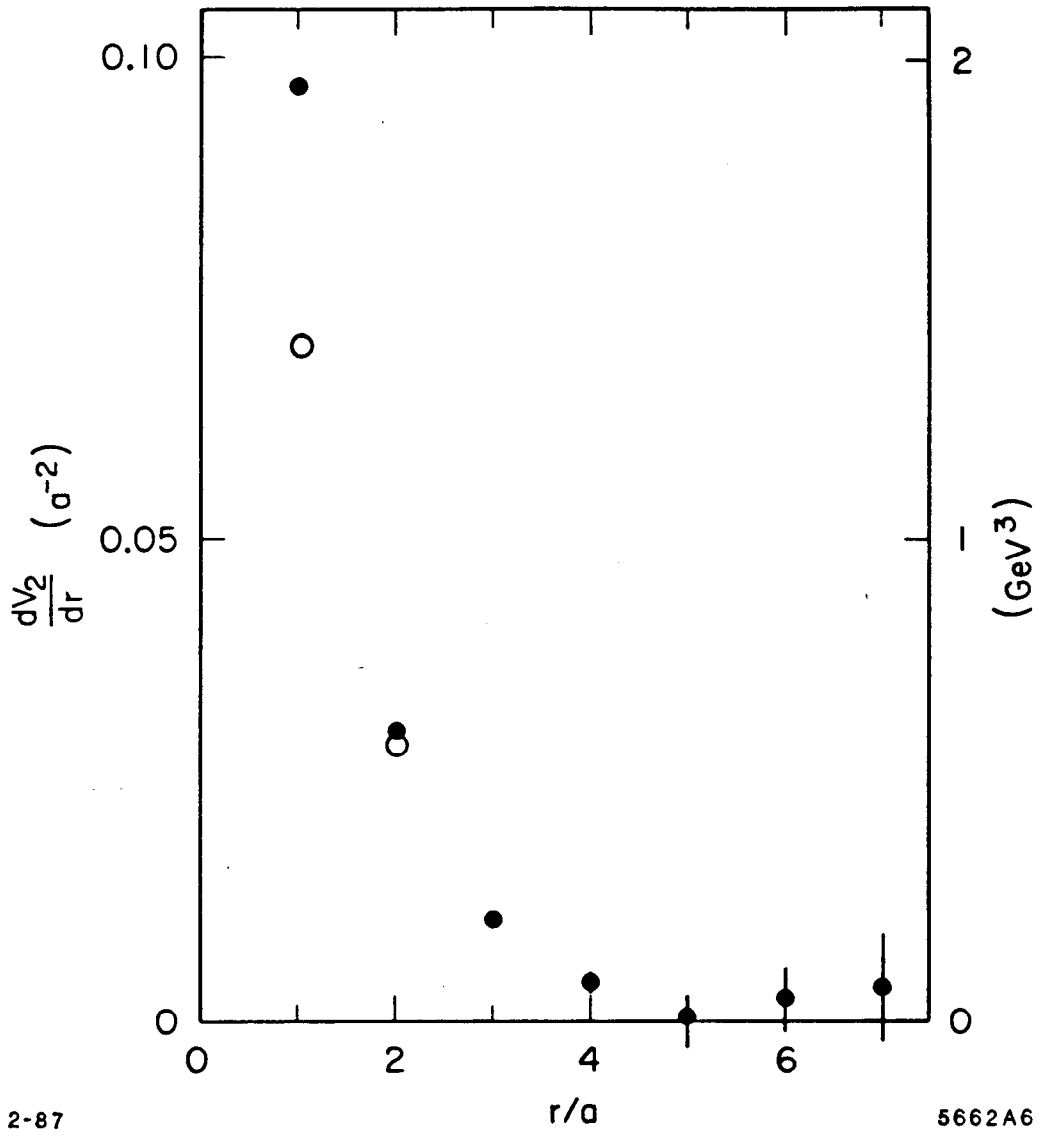

Fig. 6. Results of a lattice Monte Carlo calculation[22] of the spin-dependent potential dV_2/dr as a function of radial distance in units of the lattice spacing, a. The solid points are before, and the open points after a correction for lattice artifacts described in Ref. 22.

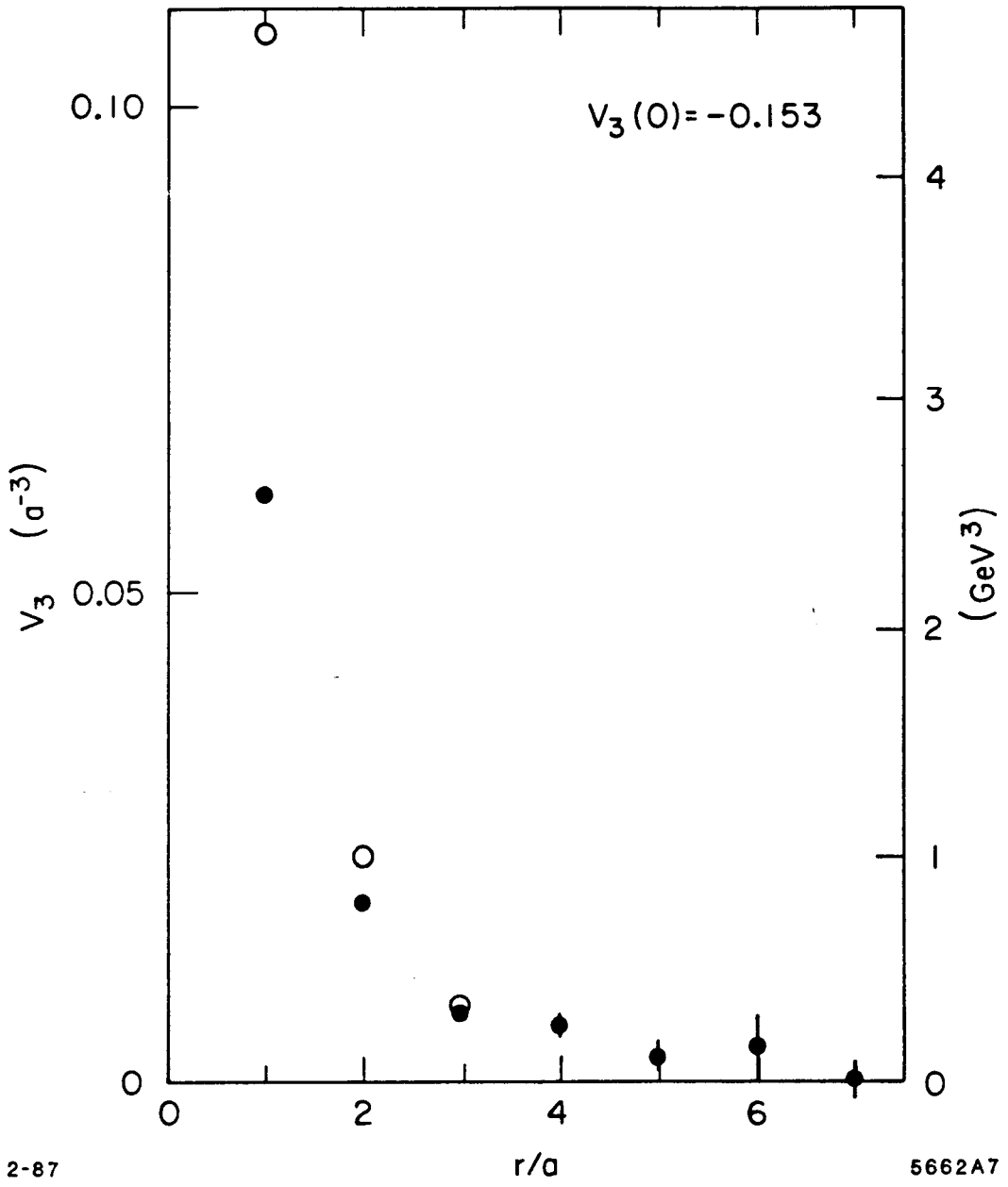

Fig. 7. Results of a lattice Monte Carlo calculation[22] of the spin-dependent potential V_3 as a function of radial distance in units of the lattice spacing, a. The solid points are before, and the open points after a correction for lattice artifacts described in Ref. 22.

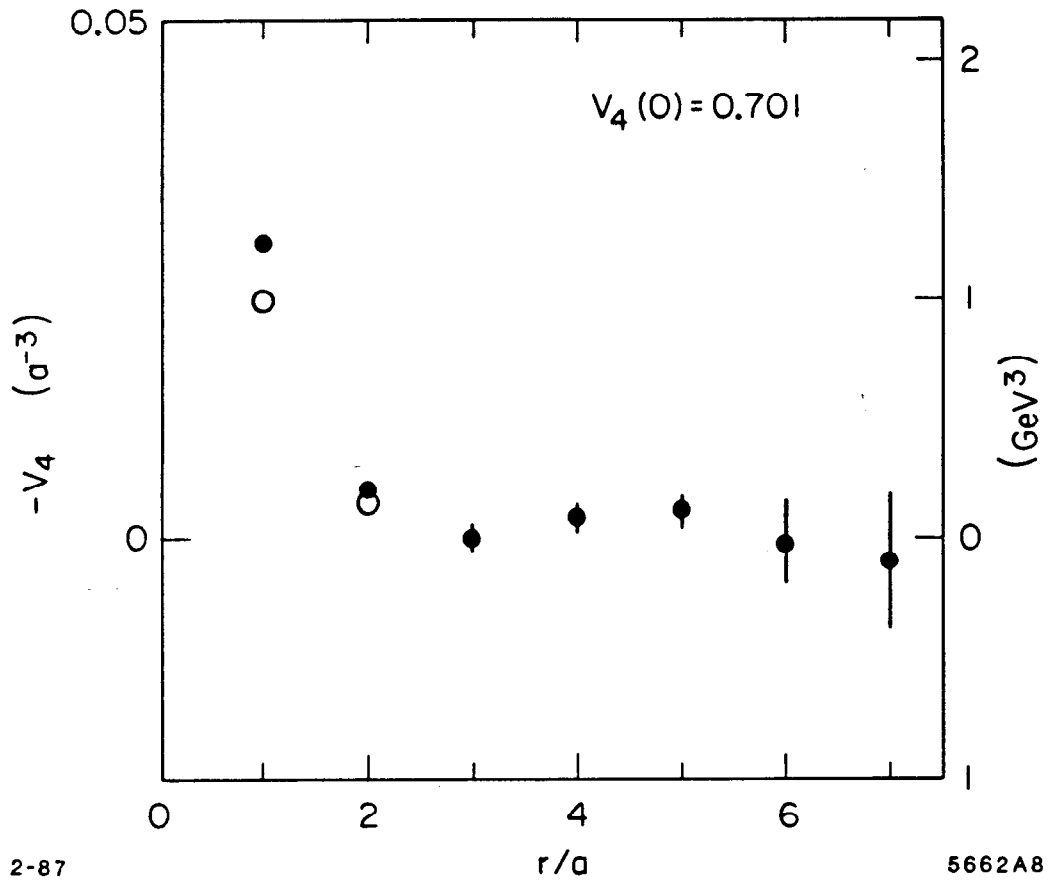

Fig. 8. Results of a lattice Monte Carlo calculation[22] of the spin-dependent potential $-V_4$ as a function of radial distance in units of the lattice spacing, a. The solid points are before, and the open points after a correction for lattice artifacts described in Ref. 22.

moment the previous discussion about the spin dependent and spin independent potentials being independent entities. Let us consider what we would obtain from a (relativistic) four-fermion interaction arising from the exchange of a vector and a scalar between a quark and the antiquark of equal mass. In momentum space this is represented by an interaction:

$$L_{int} = \widetilde{s}(q^2)\ \bar{u}u\bar{v}v + \widetilde{v}(q^2)\ \bar{u}\gamma_\mu u\bar{v}\gamma^\mu v. \tag{13}$$

If we do an expansion in powers of v^2/c^2, the static limit is the spin independent potential v + s, and the spin dependent terms give the Breit-Fermi potential, which in configuration space is:

$$\begin{aligned} V_{SD}(r) = \frac{\vec{S}\cdot\vec{L}}{2m^2}\left(-\frac{dv(r)+ds(r)}{rdr}+4\frac{dv(r)}{rdr}\right) \\ + \frac{1}{12m^2}\left(6\vec{S}\cdot\hat{r}\vec{S}\cdot\hat{r}-2\vec{S}\cdot\vec{S}\right)\left(\frac{dv(r)}{rdr}-\frac{d^2v(r)}{d^2r}\right) \\ + \frac{1}{6m^2}\left(2\ \vec{S}\cdot\vec{S}-3\right)\ \bigtriangledown^2 v(r). \end{aligned} \tag{14}$$

The term $-(dv(r) + ds(r))/rdr$ in the first line is due to the familiar Thomas precession, and it is followed by usual spin-orbit, tensor (on the second line), and spin-spin (on the third line) interactions, each with a coefficient related to v(r) or s(r).

Now we are in a position to compare what is in Eq. (14) to the generic decomposition in Eq. (12) involving V_1, V_2, and V_3. First, the spin independent potential V is here given by the sum of the vector and scalar potentials, $v + s$. Second, the spin dependent potentials V_2. V_3, and V_4 are all expressible in terms of derivatives of only the vector part of the potential, v. Hence, if v is related to

gluon exchange and its associated 1/r behavior, then the potentials V_2, V_3, and V_4 are all short range in character.

This encourages us to make the following division: the scalar term is long range and associated with quark confinement, while the vector term is short range (we include 1/r behavior as short range) and associated with gluon exchange. From the short range Coulomb-like piece one obtains the spin dependent terms we are long accustomed to in atomic physics: a spin-orbit interaction (minus the piece due to Thomas precession), a tensor interaction, and a spin-spin interaction. As you go to long range, the confining interaction, which is Lorentz scalar in character, becomes dominant. The associated physical picture[23] has a color flux tube that connects the quark and antiquark, and as they rotate around each other the flux tube rotates along with them. Consequently there are no spin dependent forces generated from this part of the potential, aside from the Thomas term which comes in with a minus sign and is generated from the spin rotation associated with Lorentz transforming from the center-of-mass to the quark or antiquark rest frame. So we get a simple way of understanding all the terms in Eq. (14). From now on we will take this identification of v and s seriously. Occasionally we will slip over to the stronger assumption that $s(r) \propto r$ and $v(r) \propto 1/r$, even to the point of thinking that we know the respective constants of proportionality.

- The Spin - Spin Interaction

The spin-spin interaction, which in the equal mass case takes the form

$$V_{SS} = \frac{1}{6m^2} \left(2\, \vec{S} \cdot \vec{S} - 3 \right) \; \nabla^2 \, v(r), \tag{15}$$

is the analogue for the color forces of QCD of the interaction which gives rise to

the hyperfine splittings between atomic levels. If we are brave enough to follow this analogy further and insert a 1/r behavior for $v(r)$, then since $\nabla^2(1/r) = -4\pi\delta^3(\vec{r})$, the spin-spin interaction is of very short range!

This delta function at the origin can be tested by noting that for quarkonium p-wave states, whose wave function at the origin vanishes, the expectation value of the spin-spin interaction should be zero. Therefore the center-of-gravity of the three states with total quark spin one and J = 0, 1, and 2 should be the same as the mass of the J = 1 state with quark spin zero:

$$\frac{5M_2 + 3M_1 + M_0}{9} = M_{\text{spin singlet}}. \tag{16}$$

(The p-wave states with total quark spin one are split in mass by the spin-orbit and tensor interactions, and the weighted average is just such as to cancel out these contributions).

For charmonium, the left-hand side of Eq. (16) is 3525.38 MeV, and an experiment in the last days of the ISR found a few candidate events with an average mass of 3525.4 ± 0.8 MeV.[24] For the bottomonium system, the corresponding values for the center-of-gravity are 9900.2 MeV for the 1P states and 10,261.6 MeV for the 2P states.[1] It would be very interesting to measure the mass of the corresponding singlet p wave states for bottomonium. There is a little bit of evidence from the CLEO experiment, studying $\pi\pi$ transitions from the 3S resonance, for a state a little below the 1P center-of-gravity.[25] As the $\bar{b}b$ system is more non-relativistic than $\bar{c}c$, the agreement with Eq. (16) should be excellent. Otherwise, the agreement in the charm case was an accident, and we had better take a close look at our assumptions on the short range nature of the spin-spin interaction.

Let us specialize to a system that consists of one heavy and one light quark. The assumption that $v(r)$ behaves as $1/r$ still gives a delta function at the origin in the part of the potential that gives the spin-spin interaction. Furthermore, the physical origin of this term in a quark color magnetic moment interacting with an antiquark color magnetic moment is still correct, and so it still depends inversely on the product of the quark mass and the antiquark mass (see the coefficient of V_4 in Eq. (9)). For example, the mass difference of the ground state vector and pseudoscalar states should behave as

$$M(^3S_1) - M(^1S_0) \propto \frac{|\Psi(0)|^2}{m_i m_j}. \tag{17}$$

If we use the fact that the spin-spin splitting is small and that in terms of constituent masses,

$$M(^3S_1) \sim M(^1S_0) \sim m_i + m_j, \tag{18}$$

then we can rewrite Eq. (17) in terms of mass squared,

$$M^2(^3S_1) - M^2(^1S_0) \propto \frac{m_i + m_j}{m_i m_j}|\Psi(0)|^2 \propto |\Psi(0)|^2/\mu_{ij} \tag{19}$$

and get a result that depends on the reduced mass of the quark-antiquark system.

One the other hand, in a system composed of a heavy and a light quark we have a atomic hydrogen-like situation with the heavy quark playing the role of the nucleus and the light quark primarily living at "large" distances. The corresponding wave function is determined by the long distance part of the potential which behaves as kr. However, for a potential which behaves as r^β, the

Schrodinger equation yields a scaling law that makes[26]

$$|\Psi(0)|^2 \propto \mu_{ij}^{\frac{3}{2+\beta}}.$$

Therefore, corresponding to the case at hand with $\beta = 1$,

$$|\Psi(0)|^2 \propto \mu_{ij},$$

and substituting this into Eq. (19), one finds[27,28]

$$M^2(^3S_1) - M^2(^1S_0) \sim \text{const.} \tag{20}$$

This relation is compared to experiment in Table 2. The input masses come from the Particle Data Tables[29] except for the $F - F^*$ mass splitting where the new result from the Mark III experiment reported to this meeting is used.[30]

Mass^2 Difference	Experimental value[27,28] in GeV^2
$M_\rho^2 - M_\pi^2$	0.57
$M_{K^*}^2 - M_K^2$	0.56
$M_{D^*}^2 - M_D^2$	0.55
$M_{F^*}^2 - M_F^2$	0.55
$M_{B^*}^2 - M_B^2$	0.55

Table 2. Ground State Vector - Pseudoscalar Mass^2 Differences

The $\rho - \pi$ difference is thrown in for good measure, even though it involves only light quarks. Even the $K^* - K$ case should not be in Table 2, for the strange quark is not all that heavy. Of course, they are in Table 2 because they all agree

magnificently with each other, so much the more so now that we have the new data on the $F^* - F$ mass difference. Equation (20) works far better than it should, as not only are the "heavy" quarks involved not all that heavy, but even the statement that the wave function at the origin squared is proportional to the reduced mass is only approximate. Such superb agreement must be an accident.

Now let us return to systems with two heavy quarks. There the wave functions are not determined by the linear part of the potential and Eq. (20) should not hold. (It doesn't!) But here we can be braver yet and insert $v(r) = -4\pi\alpha_s/r$ into Eq. (15) and sandwich it between ground state vector and pseudoscalar meson wave functions to obtain[31]

$$M(^3S_1) - M(^1S_0) = \frac{32\pi\alpha_s}{9} \frac{|\Psi(0)|^2}{m^2} \left(1 + O(\frac{\alpha_s}{\pi})\right), \tag{21}$$

where even the next order QCD corrections have been calculated. If we take the measured splitting between the ψ and η_c and invert Eq. (21) to find α_s, the result[31] is 0.3 to 0.4. This is perhaps a little bit too big, not to be regarded as very significant at this time.

- The Spin-Orbit and Tensor Interactions

Spin-orbit terms give rise to the fine structure in the old atomic physics terminology. In the case of equal constituent masses they take the form

$$V_{S.O.} = \frac{\vec{S}\cdot\vec{L}}{2m^2} \left(-\frac{ds(r)}{rdr} + 3\frac{dv(r)}{rdr}\right), \tag{22a}$$

and

$$V_{Tensor} = \frac{1}{12m^2}\left(6\vec{S}\cdot\hat{r}\vec{S}\cdot\hat{r} - 2\vec{S}\cdot\vec{S}\right) \left(\frac{dv(r)}{rdr} - \frac{d^2v(r)}{d^2r}\right). \tag{22b}$$

If we take the spin-orbit and tensor interactions and calculate their contri-

butions to the ${}^3P_J$ state masses, we get[32]

$$M({}^3P_2) = \vec{M} + a - 2b/5 \tag{23a}$$

$$M({}^3P_1) = \vec{M} - a + 2b \tag{23b}$$

$$M({}^3P_0) = \vec{M} - 2a - 4b, \tag{23c}$$

where the matrix elements a and b are defined as

$$a = \frac{1}{2m^2}\left\langle -\frac{ds}{rdr} + 3\frac{dv}{rdr}\right\rangle, \tag{24a}$$

$$b = \frac{1}{12m^2}\left\langle \frac{dv}{rdr} - \frac{d^2v}{dr^2}\right\rangle. \tag{24b}$$

We can summarize the relative values of the matrix elements in terms of one number by forming the ratio

$$r = \frac{M({}^3P_2) - M({}^3P)_1}{M({}^3P_1) - M({}^3P_0)} = \frac{2a - \frac{12}{5}b}{a + 6b}. \tag{25}$$

If only the spin-orbit term contributes, $r = 2$, while if the Coulomb-like vector part of the potential $v(r)$ is present, $r = 0.8$. As one turns on the scalar term, $s(r)$, the matrix element a decreases, as does r.

If you look at the experimental numbers,[1] updated with recent data, particularly from CUSB,[33] one finds[1] for charmonium $r_{\chi_c} = 0.50 \pm 0.02$, and for bottomonium $r_{\chi_b} = 0.67 \pm 0.05$ and $r_{\chi_b'} = 0.70 \pm 0.20$, for the 1P and 2P states, respectively. All these values are smaller than would result from solely a Coulomb-like vector term, and point toward a non-negligible scalar term. Moreover, the

detailed predictions from taking the vector term as $-\frac{4}{3}\alpha_s/r$ and the scalar term as kr give quite good agreement[34] with the data, particularly for bottomonium (recall that one expects some corrections, particularly for charmonium). The case is getting fairly good for a substantial part of the long range, confining part of the potential being scalar rather than vector.

For mesons composed of a heavy quark and a light antiquark or *vice versa* the physical situation is different, as we discussed previously in considering the spin-spin interaction. The light quark lives at larger distances, so that the Thomas term, $-ds(r)/rdr$, can "beat" the net vector term, $3dv(r)/rdr$, and the effect of the spin orbit interaction, $\langle V_{S.O.}\rangle$, can be reversed in sign. This would result in an inversion of spin multiplets[35] compared to atomic physics, charmonium, and bottomonium where the higher spin state lies higher: the ordering would now be $M(^3P_0) > M(^3P_1) > M(^3P_2)$. This idea might be testable in the ^3P charm meson states, labelled here D^{**}'s. A candidate state, the $D^{**}(2420)$, already has been found and must be J = 1 or 2, as it decays to $D^*\pi$. If this multiplet is inverted, the J = 0 state, which decays to $D\pi$, will lie at a higher mass than the $D^{**}(2420)$.

Conclusion

In this brief and incomplete review of the spectroscopy of heavy quark systems, we have seen that we have a good qualitative picture of the nature of the spin-independent forces. That, plus some phenomenological potentials inspired by fundamental theory, carry us a long way. For the spin-dependent effects we even have a semi-quantitative understanding, as they are more sensitive to the short distance part of the potential and we have more insight and more tools to help us sort things out.

Eventually, we want a quantitative calculation of both the spin-independent potential $V(r)$ and the spin-dependent potentials $V_2(r)$, $V_3(r)$, and $V_4(r)$, from QCD. This will likely come in due time from improvements in computer power and in technique over the present lattice calculations.

In the meantime, to clarify the emerging picture, we need more data. We need to find or confirm the $^1P_1$ states of charmonium and bottomonium. We need to find the η_b. We need to find the other D^{**}'s. And maybe best of all, we need to see the spectrum of toponium.

2. Heavy Quark Decays

Introduction

In this second lecture we turn from the spectroscopy of hadrons involving heavy quarks to their decays. This is a comparatively new subject, but one which is already in a fairly mature state experimentally:[1] we have measurements of many D meson branching ratios, including Cabibbo suppressed nonleptonic modes and the decomposition of the semileptonic decays into exclusive channels; excellent lifetime measurements exist for both charm and bottom hadrons; a good beginning has been made on the study of exclusive decays of the F, Λ_c and $B^{0,+}$.

On the theoretical side, we have a solid general framework within which to calculate these weak decays. In particular, this means starting with the electroweak interactions and their gauge group, $SU(2) \times U(1)$, and adding the corrections due to the strong interactions through the use of the renormalization group equation (or an equivalent formulation of the same physics), with anomalous dimensions computed from QCD.

These calculations are carried out at the quark level. A first stage in their application to actual hadrons is simply to neglect any other constituent of the decaying hadron aside from the heavy quark. In such a spectator model, as it is called, one directly carries over the quark level calculation to be the hadron level result, with the spectator quarks and gluons assumed to arrange themselves into the final state particles together with the quarks (or leptons) coming from the heavy quark at no cost or benefit to the overall rate.

From the present data on charmed particle lifetimes, it is clear that there are differences of a factor of two or so between different species.[1] To do better

than that, it is necessary to go beyond the spectator model and to consider not just what happens at the quark level but at the hadron level. In so doing, ideas such as annihilation diagrams, interference, color (mis)matching, and final state interactions have entered the discussion.[36]

This lecture will be a brief review of the subject of the decays of hadrons containing heavy quarks. We will start at the quark level where we will spend a large proportion of the review, since we know quite precisely how to proceed theoretically and the results give a semi-quantitative description of the experimental situation as we know it today. Then we will describe the various ideas enumerated above as corrections to the spectator model, leaving a more detailed analysis of the merits of these approaches in light of the present experimental situation to others.[37]

Weak Decays at the Quark Level

- Semileptonic Decays

It is theoretically simplest to start with semileptonic decays of the form

$$Q \to q + e\bar{\nu}_e$$

(such as $b \to ce\bar{\nu}_e$) or

$$Q \to q + \bar{e}\nu_e$$

(such as $c \to s\bar{e}\nu_e$) which correspond to a Hamiltonian density of the form

$$\mathcal{H} = -V_{Qq}\,\frac{G_F}{\sqrt{2}}\,\bar{q}\gamma_\mu(1-\gamma_5)Q\;\bar{e}\gamma^\mu(1-\gamma_5)\nu_e. \tag{26}$$

In Eq. (26) we have used particle names in place of the corresponding spinor

operators and introduced the one factor that does not enter into the analogous expression for muon decay, the Kobayashi - Maskawa factor V_{Qq}.

The corresponding decay rate can then be easily related to that for muon decay, $G_F^2 m_\mu^5/192\pi^3$:

$$\Gamma(Q \to q e \bar{\nu}_e) = |V_{Qq}|^2 \, \frac{G_F^2 M_Q^5}{192\pi^3} \, F\left(\frac{m_q}{M_Q}\right) \tag{27}$$

where

$$F(\Delta) = 1 - 8\Delta^2 + \Delta^6 - \Delta^8 - 24\Delta^4 \ell n \Delta. \tag{28}$$

Note again the extra Kobayashi - Maskawa factor in front and the phase space factor, F, which is unity for a massless final quark. This factor drops off rather quickly, so that $F(0.3) = 0.52$, a value relevant approximately for the $c \to s$ and the $b \to c$ transitions.

The electron (positron) energy spectrum is different in the two cases. For $b \to c e \bar{\nu}_e$ it is like that in muon decay and gives rise to a "hard" spectrum that does not vanish at the high energy end:

$$\frac{1}{\Gamma} \frac{d\Gamma}{dx} = \frac{12}{5} \, x^2(2 - x), \tag{29}$$

while for $c \to s \bar{e} \nu_e$ (and for $t \to b \bar{e} \nu_e$) it vanishes at the two ends

$$\frac{1}{\Gamma} \frac{d\Gamma}{dx} = 12x^2(1 - x) \tag{30}$$

and where the scaled energy variable is

$$x = \frac{2E_e}{M_Q} \leq 1 - \frac{m_q^2}{M_Q^2}. \tag{31}$$

Similar results of course hold for decays involving muons or taus.

- Nonleptonic Decays

The Hamiltonian density for nonleptonic decays such as $Q \to q + u\bar{d}$ has the same basic form,

$$\mathcal{H} = -V_{Qq} \frac{G_F}{\sqrt{2}} \bar{q}_\alpha \gamma_\mu (1-\gamma_5) Q_\alpha \; \bar{u}_\beta \gamma^\mu (1-\gamma_5) d_\beta \tag{32}$$

as for semileptonic decays, aside from the addition of the color indices α and β which are summed over the three colors to form color singlet currents. The decay rate

$$\Gamma(Q \to qu\bar{d}) = 3 \; |V_{Qq}|^2 \; \frac{G_F^2 M_Q^5}{192\pi^3} \; F\left(\frac{m_q}{M_Q}\right) \tag{33}$$

is also identical to the semileptonic case except for the factor of three on the right hand side due to color (we are neglecting the masses of the u and d quarks, just as we neglected those of the e and ν_e previously).

Now let us rewrite the Hamiltonian in a slightly different form:

$$\begin{aligned}\mathcal{H} = -V_{Qq} \frac{G_F}{2\sqrt{2}} \cdot \\ \Big[c_+ \Big[\bar{q}_\alpha \gamma_\mu (1-\gamma_5) Q_\alpha \bar{u}_\beta \gamma^\mu (1-\gamma_5) d_\beta \; + \bar{q}_\alpha \gamma_\mu (1-\gamma_5) d_\alpha \bar{u}_\beta \gamma^\mu (1-\gamma_5) Q_\beta \Big] \\ + \; c_- \Big[\bar{q}_\alpha \gamma_\mu (1-\gamma_5) Q_\alpha \bar{u}_\beta \gamma^\mu (1-\gamma_5) d_\beta \; - \bar{q}_\alpha \gamma_\mu (1-\gamma_5) d_\alpha \bar{u}_\beta \gamma^\mu (1-\gamma_5) Q_\beta \Big] \Big]\end{aligned} \tag{34}$$

with $c_+ = c_- = 1$ initially. All we have done is to add and subtract a term which is nothing but the original expression with $Q \leftrightarrow q$. Moreover, this term would be identical to the original one if it were not for the presence of the color indices; without them the interchange $Q \leftrightarrow q$ is a Fierz transformation under which $V-A$ interactions go into themselves. In the decay rate, the three on the

right-hand side of Eq. (33) is replaced by $2c_+^2 + c_-^2$, which again is no change at all when $c_+ = c_- = 1$.

So why make a more complicated expression out of something simple? The answer lies in what happens when we turn on the strong interactions and add the effects of QCD to the purely weak interactions that we have considered up to this point. The weak interaction will be modified by the presence of strong interaction effects and c_+ and c_- will be renormalized. But they have been carefully chosen in this regard, for they only go into themselves under this renormalization, i. e. the corresponding operators, which are even or odd under interchange of color indices, do not mix through QCD corrections. Not only do the strong interactions modify c_+ and c_- from their initial value of unity, but they introduce new operators into the effective Hamiltonian. These so-called "penguin" operators, which come in beginning at the one loop level, have a different space-time structure than the $V - A \times V - A$ structure we have had up to now. We proceed to consider each of these effects and their magnitude in turn.

- The Calculation of c_+ and c_-

To calculate what happens to c_+ and c_- under renormalization due to QCD is equivalent to being able to study their behavior as one moves from one momentum scale to another. More specifically, at the momentum scale corresponding to M_W the weak interactions are characterized by the "bare" Hamiltonian density of Eq. (31) and $c_+ = c_- = 1$. We are interested in what happens when we move down to a momentum scale characteristic of hadrons, i.e. roughly the mass of the decaying heavy quark.

The study of what happens when one moves from one momentum scale to another is directly formulated through a renormalization group equation. In the

case of c_+ and c_-, they satisfy such an equation of the form:

$$\left[\mu\frac{\partial}{\partial\mu} + \beta(g)\frac{\partial}{\partial g} - \gamma_\pm(g)\right]c_\pm(q/\mu, g) = 0, \tag{35}$$

where μ is some reference scale of momentum (the renormalization point) and q is a second scale at which we wish to calculate the effective weak Hamiltonian. In this equation, $\beta(g)$ is the standard beta function of the theory,

$$\beta \equiv \mu\frac{\partial g}{\partial\mu},$$

which characterizes how the coupling changes with a change of scale. For QCD, it has the perturbation theory expansion,

$$\beta(g) = \frac{g^3}{48\pi^2}(2n_f - 33) + ... \tag{36}$$

where n_f is the number of quark flavors. Notice that the coefficient of g^3 is negative as long as $33 > 2n_f$. In other words, the coupling decreases as we increase the scale of momentum at which we are looking. This is just the property of asymptotic freedom; the theory of QCD becomes more and more like a free field theory as we increase the momentum scale. The quantities $\gamma_\pm$ are the anomalous dimensions associated with the operators $c_\pm$, respectively. They also can be calculated in a perturbative expansion, starting in order g^2, where they originate in graphs where a single gluon is exchanged between fermion lines in the basic four-fermion weak interaction:[38]

$$\gamma_+ = +\frac{g^2}{4\pi} + ... \tag{37a}$$

$$\gamma_- = -\frac{g^2}{2\pi} + ... \tag{37b}$$

Note that if $\gamma_\pm = 0$, then the combination of derivatives on the left-hand side of

the renormalization group equation can be rewritten as a total derivative:

$$\left[\mu\frac{\partial}{\partial\mu} + \beta(g)\frac{\partial}{\partial g}\right] c_\pm(q/\mu, g) = \left[\mu\frac{d}{d\mu}\right] c_\pm = 0, \tag{38}$$

simply expressing the fact that $c_\pm$ does not change under a change of momentum scale if the anomalous dimensions are zero. In the case at hand, as we have just seen, the anomalous dimensions are non-zero and the operator coefficients $c_\pm$ change with scale.

We now proceed to solve this renormalization group equation.[39] The method of solution that follows at first looks like it is pulled out of the hat, but we will see the rationale for it, so bear with me for a moment.

We begin by defining the quantity $\bar{g}$ through an integral:

$$\ln(q/\mu) \equiv \int_g^{\bar{g}(q/\mu,g)} \frac{dx}{\beta(x)} \tag{39}$$

with $\bar{g}(1,g)$. The quantity $\bar{g}$, which is dimensionless, can only be a function of the ratio of the momentum scales q and μ and the coupling g at the reference scale μ; it is just the "running coupling" that is familiar to all of us. To see this, let us put it in a more familiar form by looking at the situation when $\bar{g}$ is small, so that we can use the perturbative result for $\beta(x) = \frac{x^3}{48\pi^2}(2n_f - 33) + ...$ under the integral in Eq. (39). If we take the first term in this expansion we obtain on performing the integral,

$$\ln q/\mu = \frac{48\pi^2}{2n_f - 33}\frac{1}{2}\left(\frac{1}{g^2} - \frac{1}{\bar{g}^2}\right) \tag{40}$$

or

$$\alpha_s(q^2) \equiv \frac{\bar{g}^2}{4\pi} = \frac{\alpha_s(\mu^2)}{1 + \frac{33-2n_f}{12\pi}\alpha_s(\mu^2)\ln q^2/\mu^2}. \tag{41}$$

This is the standard expression for the running of α_s when it is small.

The definition of $\bar{g}$ in Eq. (39) is perfectly general though; it simply reduces to the standard form in the small coupling region upon using lowest order perturbation theory for $\beta(x)$. Moreover, it is relevant to solving our equation since it exactly satisfies the renormalization group equation with zero anomalous dimensions:

$$\left(\mu\frac{\partial}{\partial\mu}+\beta(g)\frac{\partial}{\partial g}\right)\bar{g}(q/\mu,g)=0, \tag{42}$$

as may be seen by applying the differential operator on the left-hand side of this equation to both sides of Eq. (39).

Now we are ready to solve the full equations for $c_\pm$. The solution of Eq. (35) is:

$$c_\pm(q/\mu,g)=c_\pm(1,\bar{g})\exp\left(\int_g^{\bar{g}}-\frac{\gamma_\pm(x)dx}{\beta(x)}\right), \tag{43}$$

as can be seen directly by substitution and employing Eq. (42) together with the fact that the derivative of an integral with respect to its upper limit of integration is just the integrand evaluated at that point.

We go again to perturbation theory to evaluate the integral in the exponent of Eq. (43):

$$\int_g^{\bar{g}}-\frac{\gamma_+(x)dx}{\beta(x)}=\frac{6}{33-2n_f}\ln\frac{\bar{g}^2}{g^2}. \tag{44}$$

Therefore,

$$c_+(q/\mu,g)=c_+(1,\bar{g})\left(\frac{\bar{g}^2}{g^2}\right)^{\frac{6}{33-2n_f}}, \tag{45}$$

and similarly,

$$c_-(q/\mu, g) = c_-(1, \bar{g}) \left(\frac{\bar{g}^2}{g^2} \right)^{\frac{-12}{33 - 2n_f}}. \tag{46}$$

We are interested in what happens between a momentum scale which is characteristic of the decaying hadron (which we take to be μ) and the weak scale, M_W (which we take to be q). Moreover, if we had also taken our reference momentum scale μ to be the weak scale, our coefficients should make the Hamiltonian density correspond to the "bare" density in Eq. (34), *i. e.*, $c_\pm(1, \bar{g}) = 1$. Therefore,

$$c_+(M_W/\mu, g) = \left(\frac{\alpha_s(M_W^2)}{\alpha_s(\mu^2)} \right)^{\frac{6}{33 - 2n_f}} \tag{47}$$

and

$$c_-(M_W/\mu, g) = \left(\frac{\alpha_s(M_W^2)}{\alpha_s(\mu^2)} \right)^{\frac{-12}{33 - 2n_f}}. \tag{48}$$

This is our sought after result for the QCD renormalization of the coefficients $c_\pm$.

When we recall that $\alpha_s(q^2)$ runs down as the momentum scale goes up, we see that $c_+(M_W/\mu, g) < 1$ and $c_-(M_W/\mu, g) > 1$. In fact, there is the simple relation

$$c_+^2 c_- = 1 \tag{49}$$

(which is traceable to the factor of -2 between the anomalous dimensions of the corresponding operators), so that one of the corresponding terms in the weak Hamiltonian is necessarily suppressed if the other is enhanced by the effects of QCD.

- Penguins

Before using these results to look at the overall picture of decays in the spectator model, let us take a brief look at the additional operators introduced by QCD, the "penguins". A set of lowest order graphs which contribute to the existence of "penguin" operators relevant to various quark decays is shown in Figure 9.

On the upper left is a one loop, "penguin" graph relevant to strange quark decay (and in particular, to neutral K decay). Once the loop integral is performed this diagram contributes to an effective operator whose space-time structure is $(V-A)\times V$, or equivalently a mixture of $(V-A)\times(V-A)$ and $(V-A)\times(V+A)$. The latter operator has a structure that is not in the original weak Hamiltonian density. Arguments have been made that although its relative coefficient is small, the corresponding operator has a big matrix element in K decays and that it contributes a large part of the experimentally observed amplitude.[40] This is a subject still very much under debate.[41]

The diagram on the upper right shows a potential "penguin" in Cabibbo suppressed charm decays. Estimates generally put its strength well below that from ordinary graphs which contribute to the same process.

In bottom decay, however, it may be possible to have processes (Cabibbo suppressed to be sure) where "penguin" diagrams give rise to contributions comparable to, or maybe even larger than, those of ordinary tree level graphs.[42] The bottom portion of Figure 9 shows a possible example. The "penguin" diagram on the lower left contributes an effective Hamiltonian density:

$$\mathcal{H} = \frac{G_F}{\sqrt{2}}\frac{\alpha_s}{3\pi}\, V_{tb}\, V_{ts}^*\, \ln(m_t^2/m_c^2)\, \bar{s}\gamma_\mu(1-\gamma_5)b\bar{u}\gamma^\mu u, \qquad (50)$$

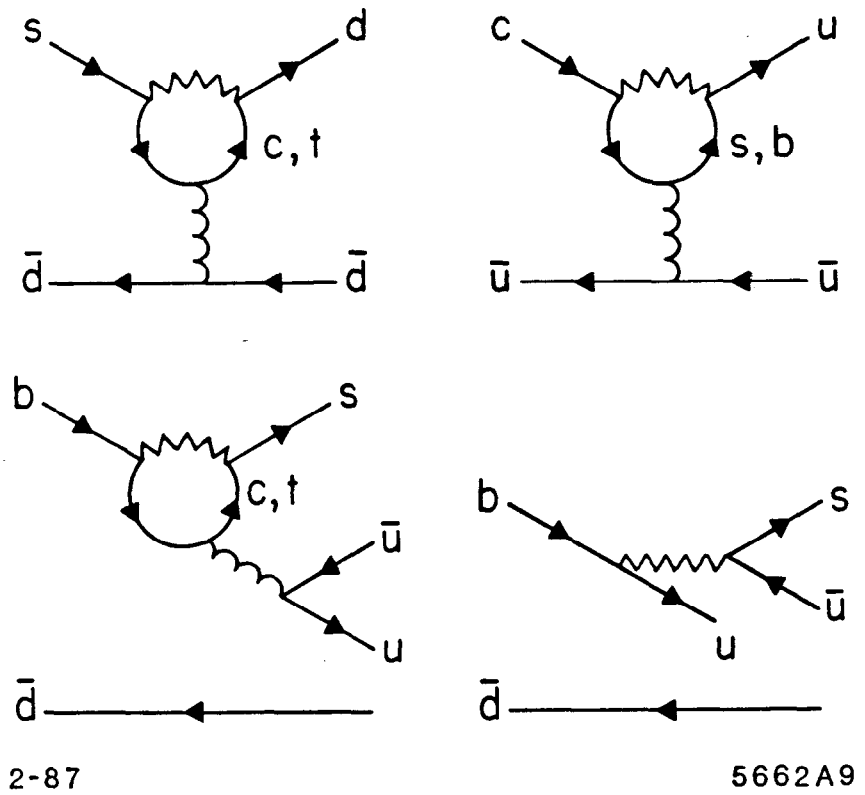

Fig. 9. Set of lowest order "penguin" graphs contributing to strange quark decay (upper left), Cabibbo suppressed charm quark decay (upper right), and Cabibbo suppressed bottom quark decay (lower left). Also shown is a spectator graph which also contributes to Cabibbo suppressed bottom quark decays (lower right).

whereas the usual spectator diagram corresponds to

$$\mathcal{H} = \frac{G_F}{\sqrt{2}} V_{ub} V_{us} \bar{u}\gamma_\mu(1-\gamma_5)b \; \bar{s}\gamma^\mu(1-\gamma_5)u. \tag{51}$$

The "penguin" loses to the spectator graph because of the $\frac{\alpha_s}{3\pi}\ln(m_t^2/m_c^2)$ that arises from having one loop and the presence of the gluon, but it wins because of the Cabibbo (or more exactly, Kobayashi-Maskawa) factor $V_{tb}V_{ts}^*$, which involves zero and one generation jumps, as compared to $V_{ub}V_{us}$, which involves two and one generation jumps, respectively. Depending in part on how small V_{ub} is (something still not known), it could well be that the spectator is the lesser of the two contributions. Then, for example, in the decays $B_d \to K^+\pi^-$ or $B_s \to \phi K^0$ the "penguin" contribution may be dominant.[43]

- Decays in the Spectator Model

What does all this mean numerically for the decay of the various quark flavors? First consider the strange quark. The statement that $c_- > 1$ corresponds to the enhancement of the $\Delta I = 1/2$ amplitude in strange particle decay, which is what one desires in order to be in accord with experiment. However, it already requires some stretching to get a factor of 3 or 4 in the amplitude, while what is needed is something like a factor of 20. Another piece of physics, perhaps "penguins" (see the discussion above), is required in addition to the QCD enhancement of c_-.

For the charm quark, if we set $\mu = m_c$, we find $c_- \sim 2$ and $c_+ \sim 1/\sqrt{2}$. At the quark level the Cabibbo allowed decay channels are $c \to s\bar{e}\nu_e$, $c \to s\bar{\mu}\nu_\mu$, and $c \to s\bar{d}u$. In the spectator model, all charmed hadrons would have the same lifetime and the same semileptonic branching fraction, which would be identified

with that for the charm quark as if it decayed in isolation from other hadronic constituents:

$$BR_{\text{semileptonic}} \sim \frac{1}{2 + 2c_+^2 + c_-^2} \sim 14\%. \tag{52}$$

For the bottom quark, with $\mu = m_b$, the QCD enhancement (suppression) of c_- (c_+) is less than that for charm: $c_- \sim 1.5$ and $c_+ \sim 0.8$. In this case we have an expanded list of decay channels at the quark level: $b \to ce\bar{\nu}_e$, $b \to c\mu\bar{\nu}_\mu$, $b \to c\tau\bar{\nu}_\tau$, $b \to cd\bar{u}$, and $b \to cs\bar{c}$. We have neglected decays where the final c quark is replaced by a u quark (using the experimental result[1] that $b \to u/b \to c$ is small). The corresponding semileptonic branching ratio is

$$BR_{\text{semileptonic}} \sim \frac{1}{2.2 + 1.2(2c_+^2 + c_-^2)} \sim 15\%, \tag{53}$$

where the semileptonic decays involving $c\bar{\tau}\nu_\tau$ and $c\bar{c}s$ have been given an approximate phase space weight which is 0.2 times that for $ce\bar{\nu}_e$.

These days, everyone is quick to point out that these results do not agree with experiment, e.g., the D^0 and the D^+ lifetimes differ by a factor of two or so, the average B semileptonic branching ratio is about 12%, etc.[1] Before we go on to investigating the shortcomings of the spectator model, let me emphasize that this is not so bad – I only wish that I was able to calculate so simply everything else involving strong interactions to a factor of two or better in the rate! The spectator model does provide a very useful qualitative and even semi-quantitative basis for calculating the weak decays of heavy quarks.

With that stressed, let it also be said that we should and can do better theoretically. We shall then look beyond the spectator model at what are the effects of the other quarks and gluons present in the initial or final state.

Beyond the Spectator Model

- Leptonic Decays

The simplest decay processes that involve the erstwhile spectator quarks are those where the initial quark and antiquark in a meson annihilate to yield a purely leptonic final state; this must be a non-spectator process. The prototype for all such decays is $\pi^- \to \mu^- \bar{\nu}_\mu$, and as for the pion, the decay rate for any pseudoscalar meson P has the form:

$$\Gamma(P \to \ell \bar{\nu}_\ell) = \frac{G_F^2 \, f_P^2 \, M_P \, m_\ell^2}{8\pi} \left(1 - \frac{m_\ell^2}{M_P^2}\right)^2, \tag{54}$$

where f_P is the pseudoscalar decay constant, the analogue of f_π.

For $D^+ \to \bar{\mu}\nu_\mu$, this yields a branching ratio

$$BR(D^+ \to \bar{\mu}\nu_\mu) = 4.3 \times 10^{-3} \, \sin^2\theta_c \left(\frac{f_D}{f_K}\right)^2 \frac{\tau_{D^+}}{10^{-12} \text{ sec}}. \tag{55}$$

As we expect[44]

$$f_D \sim f_F \sim f_B \sim f_K,$$

the branching ratio for this mode is to be found down at the level of 2×10^{-4}.

The one case of a heavy meson with an appreciable leptonic branching ratio is the F (now renamed the D_s, but we retain the old name here). The particular decay of relevance is $F^+ \to \bar{\tau}\nu_\tau$, where a calculation as above gives:

$$BR(F^+ \to \bar{\tau}\nu_\tau) = 4.3 \times 10^{-2} \left(\frac{f_F}{f_K}\right)^2 \frac{\tau_{F^+}}{10^{-12} \text{ sec}}. \tag{56}$$

Here we have neither a Cabibbo nor a helicity suppression (because of the high tau mass), and given the present F lifetime[1] we can expect a branching ratio of nearly 2%.

In the case of a vector meson decaying weakly to leptons, we no longer have the helicity suppression and the rate does not involve a factor of m_ℓ^2:

$$\Gamma(V \to \ell\bar{\nu}_\ell) = \frac{G_F^2 f_V^2 M_V^3}{24\pi}\left(1 - \frac{m_\ell^2}{M_V^2}\right)^2 \left(2 + \frac{m_\ell^2}{M_V^2}\right). \tag{57}$$

However, for all the known vector mesons, such a mode is swamped by strong or electromagnetic decays; even for the vector meson containing a t quark it is overwhelmed by other weak decays.

- Semileptonic Decays

We have considered these decays at the quark level previously, which presumably provides an approximate, smoothed inclusive sum of the actual exclusive modes such as $D \to Ke\bar{\nu}_e$, $D \to K^* e\bar{\nu}_e$, etc. If the number of available exclusive channels is small, as in D semileptonic decay, then they can be untangled experimentally[1] and calculated individually theoretically.

Consider, for example, $D \to \bar{K}\bar{e}\nu_e$. This decay has a standard matrix element

$$\mathcal{M} = -\, V_{cs}\, \frac{G_F}{\sqrt{2}} f_+(q^2)\ (p_K^\mu + p_D^\mu)\ \bar{v}_e \gamma_\mu (1 - \gamma_5) u_\nu, \tag{58}$$

where $q = p_D - p_K$ is the four-momentum carried by the lepton pair. The corresponding rate is

$$\Gamma(D \to \bar{K}\bar{e}\nu_e) = |V_{cs}|^2\ \frac{G_F^2\ M_D^5}{192\pi^3}\ 8 \int_0^{(M_D - m_K)^2} dq^2\ |f_+(q^2)|^2\ |\vec{q}|^3, \tag{59}$$

where $|\vec{q}|$ is taken in the D rest frame. If the form factor f_+ had no q^2 dependence,

then the last integral can be done explicitly,

$$8 \int_0^{(M_D-m_K)^2} dq^2 \, |f_+(q^2)|^2 \, |\vec{q}|^3 = |f_+(0)|^2 \cdot \frac{1}{4} F(m_K/M_D). \qquad (60)$$

The function $F(\Delta = m_K/M_D)$ in Eq. (60) is just that introduced in Eq. (28) from the decay rate calculation at the quark level. In fact, the whole expression for the decay rate for the exclusive mode $D \to \bar{K}\bar{e}\nu_e$ is just $\frac{1}{4}|f^+(0)|^2$ times that for the inclusive rate at the quark level if we replace M_D and m_K by the corresponding masses of the"heavy" quarks they contain, m_c and m_s. Numerically, $F(m_K/M_D) = 0.60$, and inserting the measured behavior[1] of the form factor f_+ increases the integral by a factor of 1.3. The measured rate for this decay can be used to obtain an expression for $|V_{cs}|$ in terms of $|f_+(0)|$, since all the other quantities in Eq. (59) are known.

This calculation of exclusive channels one by one can be carried a step further by using a model of the possible final states and their matrix elements to systematically calculate semileptonic decays as a sum of exclusive channels. Such a calculation has recently been carried out using the quark model for the final state resonances and their matrix elements,[45] with results for the electron energy spectrum in D meson decay as shown in Figure 10. A comparison is also made there of the sum of the exclusive channels and the inclusive decay calculated at the quark level. The overall rates (integrated area under the curves) in the two cases are quite close in value, while the exclusive calculation gives a somewhat softer electron spectrum. A similar comment holds for B decay into charm, as shown in Figure 11. When it comes to B decay into non-charmed final states however, the sum of the exclusive channels involving comparatively low-lying final states which is shown in Figure 12 falls well short of giving the same rate as

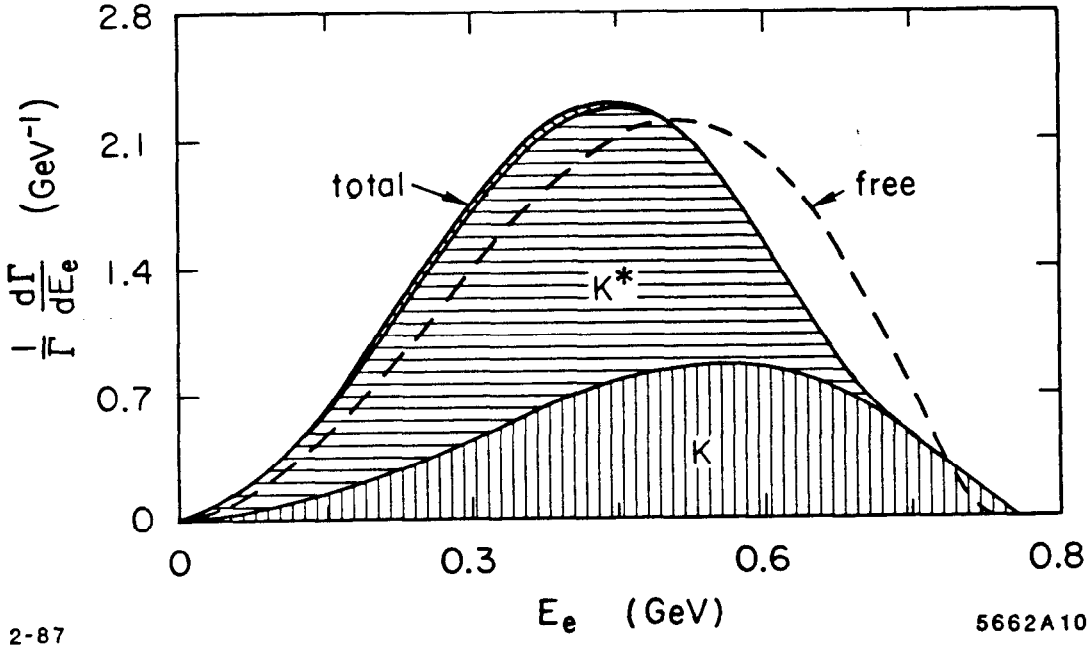

Fig. 10. The components of the electron spectrum from different hadronic channels in semileptonic D decays involving strange meson final states according to Ref. 45.

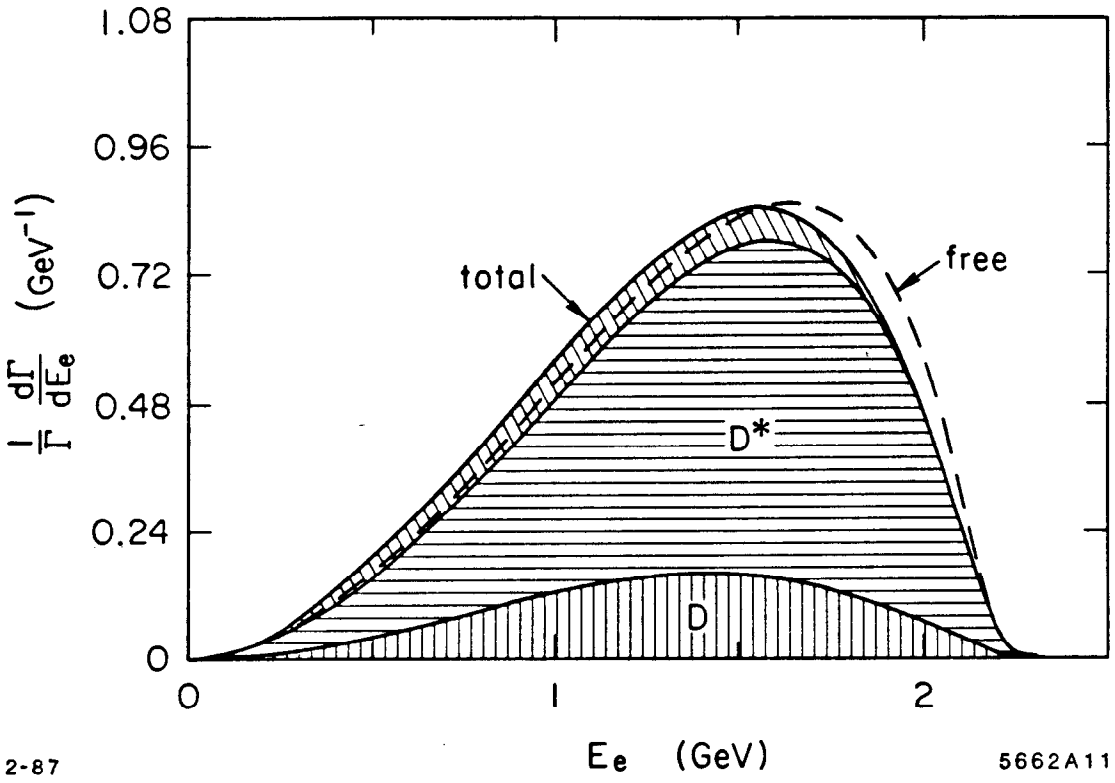

Fig. 11. The components of the electron spectrum from different hadronic channels in semileptonic B decays involving charmed meson final states according to Ref. 45.

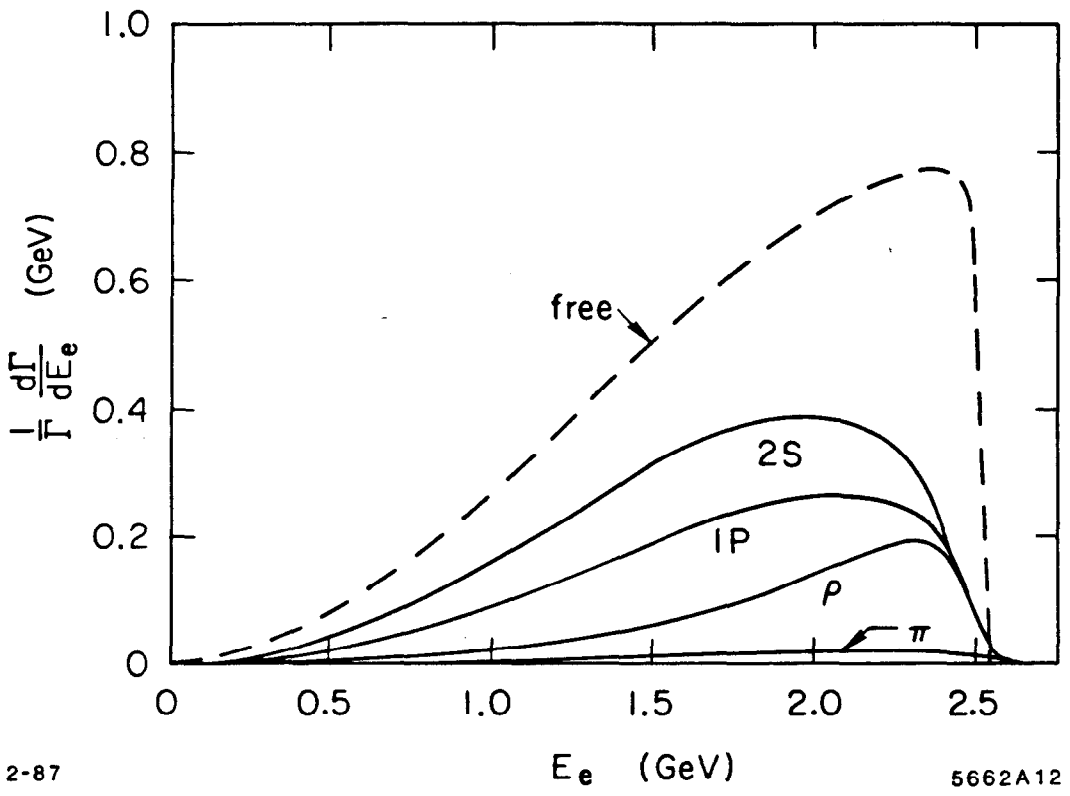

Fig. 12. The components of the electron spectrum from different hadronic channels in semileptonic B decays involving non-charmed meson final states according to Ref. 45.

the inclusive decay calculated at the quark level. It yields a much softer electron energy spectrum as well. Usually, it is precisely near the endpoint of the spectrum where one would tend to trust the calculation involving a discrete sum of exclusive states, as opposed to the quark level calculation, which at best can be a smooth averaging of the discrete sum. It is also the shape of the spectrum near the endpoint which is critical in sorting out $b \to u$ from $b \to c$. The decidedly softer spectrum in Figure 12 for the former process makes experiment less sensitive to $b \to u$; there are less restrictive limits on $b \to u$ when the data are analyzed in terms of it.

- Nonleptonic Decays

There are a number of ways that have been proposed to account for the deviations from the spectator model in nonleptonic decays. We examine them briefly in this section.[36,37]

Final State Interactions

Once created by the weak interaction, the final hadrons undergo strong interaction scattering effects. If the pair of hadrons has an energy which is below inelastic threshold for that channel, it can be proven rigorously that the amplitude must have the phase of the elastic scattering process characterized by the appropriate quantum numbers at that energy.[46] For a process in which the final state is composed, for example, of two possible isospins, the corresponding portions of the weak amplitude each pick up a final state interaction factor with a phase that is appropriate to scattering in that particular isospin state. Such phases can completely change predictions made for the weak amplitudes alone by destroying the phase relationship between different amplitudes. For example, consider the decay $D^0 \to \bar{K}^0\pi^0$ in which the final $K\pi$ system has isospin 1/2 or

3/2:

$$A(D^0 \to \bar{K}^0\pi^0) = \sqrt{\frac{1}{3}}A_{1/2} + \sqrt{\frac{2}{3}}A_{3/2}. \tag{61}$$

As we will see shortly, this amplitude is predicted to be very small due to color mismatches in one picture of such decays. If this is recast in terms of the isospin decomposition of Eq. (61), the small net amplitude must come about when

$$A_{1/2} \sim -\sqrt{2}\, A_{3/2}. \tag{62}$$

Once we add final state interactions, the same decay amplitude becomes

$$A(D^0 \to \bar{K}^0\pi^0) = \sqrt{\frac{1}{3}}A_{1/2}e^{i\delta_{1/2}} + \sqrt{\frac{2}{3}}A_{3/2}e^{i\delta_{3/2}}, \tag{63}$$

where we have used a simple phase factor to represent the final state interactions, even though one is well above the inelastic threshold for $K\pi$ scattering at the energy of the D. Even with this somewhat symbolic notation, the point is well made[47] that with sizable strong interaction phases of opposite sign, the cancellation between the two terms on the right-hand side of Eq. (61) can be turned around into a positive enhancement, totally obscuring the underlying relation obtained from the weak interactions alone. Even more, strong interaction rescattering can produce a final state that is not allowed in a particular model from weak processes alone. Such is the case for the process $D^0 \to \bar{K}^0\phi$, which is not permitted to occur through the weak interactions without the presence of annihilation graphs (see below), but could occur through the chain[48]

$$D^0 \to \bar{K}^{*0}\eta \to \bar{K}^0\phi, \tag{64}$$

where the first step is already allowed in the spectator model and the second step is a purely strong interaction rescattering process.

Color Factors and (mis)Matching

Consider a quark level process like $c_\alpha \to s_\alpha + \bar{d}_\beta u_\beta$, where color indices have been reinstated (and where repeated, they are summed over the three colors), that takes place inside a D^0 meson with quark content $c_\alpha \bar{u}_\alpha$. If we proceed naively to form final hadrons out of the resultant quarks and antiquarks, then the color indices for the combination $(u\bar{d})(s\bar{u})$, e.g., $\pi^+ K^-$, automatically "match" to form color singlet hadrons. The color indices for $(u\bar{u})(s\bar{d})$, e.g., $\pi_0 \bar{K}^0$, are mismatched: Only one time in three are the indices appropriate for forming a color singlet. Thus we expect that the second process will be down a factor of 9 from the first. Actually the prediction is[49]

$$\frac{\Gamma(D^0 \to \bar{K}^0 \pi^0)}{\Gamma(D^0 \to K^- \pi^+)} = \frac{1}{18}, \tag{65}$$

because there is an additional factor of one-half coming from the square of the π^0 wave function, $\frac{1}{\sqrt{2}}(\bar{u}u - \bar{d}d)$. When the usual QCD corrections are put in, the prediction is reduced further to $\sim 1/40$. This (and other cases of such color suppression) is in gross disagreement with experiment,[1] where these two widths are within a factor of two of each other. The color matching or mismatching can be destroyed if we allow soft gluons to transfer color from one final quark to another at no cost in rate. However, there may be a modified version of such color factors that is of relevance, and indeed they play a role in some of the recent attempts to understand D decays systematically.[50,51]

Interference

Unlike the example above where the two different ways of combining final quarks and antiquarks led to two distinct hadronic final states, there are cases

where the final state hadrons are the same. An example of this is given in Figure 13, where the two ways of combining the final quarks in D^+ decay, say into two pseudoscalar mesons, leads to the same final state, i. e., $\bar{K}^0\pi^+$. By the laws of quantum mechanics the amplitudes are coherent, and in this particular case are found to interfere destructively. This reduces (at least this) particular partial width and it can be argued that this is a mechanism for reducing the total width of the D^+ and hence increasing its lifetime and semileptonic branching fraction as compared to the D^0 and F^+, for which this interference does not occur (in the Cabibbo allowed decays).[52,53] This mechanism seems to be present at some level, although it has been argued that it is probably not enough of an effect by itself to give a factor of two difference in the D^+ and D^0 lifetimes.[54]

Annihilation

Graphs like those in Figure 14 are suppressed for the decays of a pseudoscalar meson into light final fermions because of the $V-A$ character of the weak interaction. This is precisely the same physics that gives the factor of m_ℓ^2 in Eq. (54) and causes the amplitudes for $\pi^- \to e\bar{\nu}_e$ and $K^- \to e\bar{\nu}_e$ to be suppressed by a factor of m_e/m_μ compared to $\pi^- \to \mu\bar{\nu}_\mu$ and $K^- \to \mu\bar{\nu}_\mu$; we sometimes say the former processes are "helicity suppressed" compared to the latter.

In the case of hadronic decays as in Figure 14, this suppression may be removed by emitting gluons. Consider, for example, the annihilation diagram for F decay in Figure 14, where a gluon is radiated by the c or $\bar{s}$ quark in the initial state, or where the gluon is present as a constituent to from the beginning.[55–57] At the vertex where the $c\bar{s}$ pair annihilate into a W they are no longer in a spin zero state (in fact, they are necessarily have spin one); the helicity suppression is gone. The width of hadrons for which such a process can contribute to the

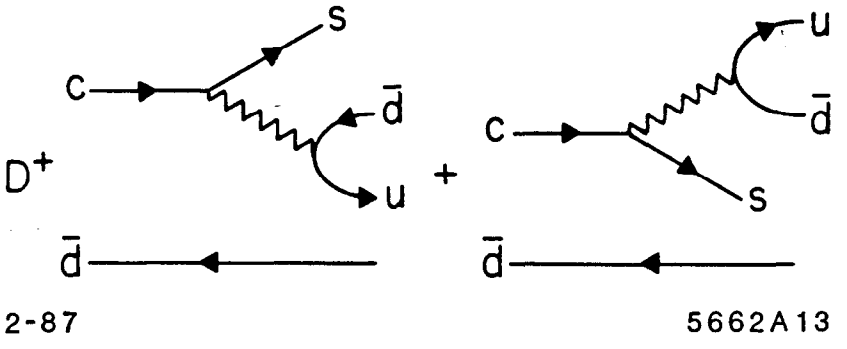

Fig. 13. Diagrams contributing to $D^+ \to \bar{K}^0\pi^+$ decay, illustrating potential interference between amplitudes arising from two different ways of combining final quarks into the same final state hadrons.

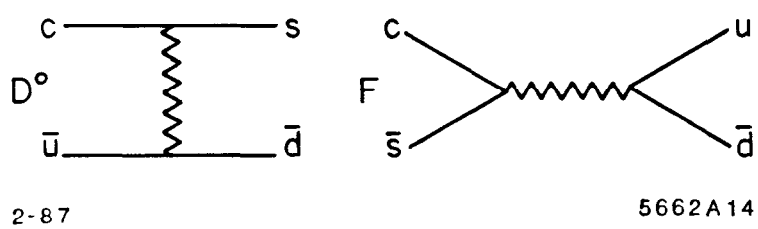

Fig. 14. Annihilation graphs contributing to D^0 and F^+ decay.

weak decays will increase; the only question is the magnitude of the effect. In particular, the width of the D^0 and F^+ should increase, while that for the D^+ should not in the dominant Cabibbo-allowed modes (but the annihilation graph does contribute to Cabibbo-suppressed modes of the D^+). In addition, specific exclusive hadronic modes, like $D^0 \to \bar{K}^0\phi$ and F decay to hadrons not containing strange quarks, are permitted through the annihilation graph and not through the spectator graph by itself (without final state interactions, see above).

There is increasing evidence that annihilation graphs do contribute to a measurable fraction of D decays. We very much need further quantitative calculations and experimental measurements of D and F decay with which to compare them. Even if such effects are important in D and F decay, they should be much less so in B decay, and this needs experimental checking as well. So while the situation with weak decays of hadrons containing heavy quarks is getting clearer, and we do have a semi-quantitative theory/model of these processes, much remains to be done both theoretically and experimentally.

REFERENCES

1. R. Schindler, lectures at this Summer Institute reviews much of the data relevant to the discussion here. See also, S. Cooper, rapporteur's talk at the XXIII International Conference on High Energy Physics, Berkeley, July 16 - 23, 1986 and SLAC preprint SLAC-PUB-4139, 1986 (unpublished).

2. Recent reviews are to be found in A. Martin, Comm. Nucl. Part. Phys. 16, 249 (1986) and W. Kwong, J. L. Rosner, and C. Quigg, University of Chicago preprint EFI 86-60, 1986 (to be published in Ann. Rev. Nucl. Part. Sci 37, 1987.

3. The basics and earlier accomplishments of lattice QCD calculations are set out in M. Creutz, *Quarks, Gluons, and Lattices* (Cambridge University Press, Cambridge, 1983).

4. S. Capstick, N. Isgur, and J. Paton, Phys. Lett. 175B, 457 (1986).

5. Relativistic corrections have been considered, for example, by P. Moxhay and J. L. Rosner, Phys. Rev. D28, 1132 (1983) and by R. McClary and N. Byers, Phys. Rev. D28, 1692 (1983). The effects of light quark pairs are studied by N. Byers and V. Zambetakis, invited talk at the Second Conference on Interactions Between Particle and Nuclear Physics, Lake Louise, Canada, May 23-32, 1986 and UCLA preprint UCLA/86/TEP/24, 1986 (unpublished).

6. The sum rule approach is reviewed by L. J. Reinders, H. Rubinstein, and S. Yazaki, Phys. Rep. 127, 1 (1985); and by M. A. Shifman, Ann. Rev. Nucl. Part. Sci 33, 199 (1984).

7. J. D. Jackson, *Proceedings of the Summer Institute on Particle Physics*,

SLAC Report No. 198, edited by M. C. Zipf (SLAC, Stanford, 1976), p. 147.

8. E. Eichten *et al.*, Phys. Rev. D17, 3090 (1978) and D21, 203 (1980).
9. J. L. Richardson, Phys. Lett 82B, 272 (1979).
10. W. Buchmuller, G. Grunberg, and S. H. H. Tye, Phys. Rev. Lett. 45, 103 (1980); W. Buchmuller and S. H. H. Tye, Phys. Rev. D24, 132 (1981).
11. A. Martin, Phys. Lett. 93B, 338 (1980).
12. H. B. Thacker, C. Quigg and J. L. Rosner, Phys. Rev. D18 274 (1978) and D21, 234 (1980); C. Quigg and J. L. Rosner, Phys. Rev. D23, 2625 (1981).
13. B. Baumgartner, H. Grosse, and A. Martin, Phys. Lett. 146B, 363 (1984).
14. B. Baumgartner, H. Grosse, and A. Martin, Nucl. Phys. B254, 528 (1985).
15. P. J. Franzini and F. J. Gilman, Phys. Rev. D32, 237 (1985).
16. G. G. Athanasiu, P. J. Franzini, and F. J. Gilman, Phys. Rev. D32, 3010 (1985).
17. E. Eichten and F. Feinberg, Phys. Rev. D23, 2724 (1981).
18. E. Eichten, *Proceedings of the 11th SLAC Summer Institute on Particle Physics*, SLAC Report NO. 267, edited by P. M. McDonough (SLAC, Stanford, 1983), p. 497.
19. M. Peskin, *Proceedings of the 11th SLAC Summer Institute on Particle Physics*, SLAC Report NO. 267, edited by P. M. McDonough (SLAC, Stanford, 1983), p. 151.
20. D. Gromes, Z. Phys. C26, 401 (1984).
21. P. de Forcrand and J. D. Stack, Phys. Rev. Lett. 55, 1254 (1985); C. Michael, Phys. Rev. Lett. 56, 1219 (1985).

22. M. Campostrini, K. Moriarty, and C. Rebbi, Phys. Rev. Lett. 57, 44 (1986).

23. W. Buchmuller, Phys. Lett. 112B, 479 (1982). See also J. L. Rosner, J. de Phys. 46, C2, Supp. 2 (1985); R. D. Pisarski and J. D. Stack, Fermilab preprint FERMILAB-PUB-86/122-T, 1986 (unpublished), and M. G. Olsson and C. J. Suchyta, University of Wisconsin preprint MAD/PH/312, 1986 (unpublished).

24. C. Baglin *et al.*, Phys. Lett. 171B, 135 (1986).

25. T. Bowcock *et al.*, Phys. Rev. Lett. 58, 307 (1987).

26. C. Quigg and J. L. Rosner, Comm. Nucl. Part. Phys. 8, 11 (1978).

27. M. Frank and P. J. O'Donnell, Phys. Lett. 157B, 174 (1985).

28. H. J. Schnitzer, Phys. Lett. 134B, 253 (1984) and Brandeis preprint, 1985 (unpublished).

29. Particle Data Group, Phys. Lett. 170B, 1 (1986).

30. W. Toki, these Proceedings.

31. W. Buchmuller, Y. J. Ng, and S. H. H. Tye, Phys. Rev. D24, 3003 (1981); A. Martin and J. M. Richard, Phys. Lett. 115B, 323 (1982).

32. J. L. Rosner, *Proceedings of the 1985 Symposium on Lepton and Photon Interactions at High Energies*, edited by M. Konuma and K. Takahashi (Kyoto University, Kyoto, 1986), p. 448.

33. P. M. Tuts, these Proceedings.

34. See Table X of Ref. 1 and references to the original calculations there.

35. H. J. Schnitzer, Phys. Lett. 76B, 461 (1978). See also, J. L. Rosner, Comm. Nucl. Part. Phys. 16, 109 (1986).

36. Some recent reviews from various viewpoints are found in A. J. Buras, Max Planck Institute preprint MPI-PAE/PTH 40/86, 1986 (unpublished); R. Ruckl, DESY preprint DESY 86/116, 1986 (unpublished); I. Bigi, Phys. Lett. 169B, 101 (1986).

37. A more complete update of the present situation is found in Ref. 36 and in I. Bigi, these Proceedings.

38. M. K. Gaillard and B. W. Lee, Phys. Rev. Lett. 33, 108 (1974); G. Altarelli and L. Maiani, Phys. Lett. 52B, 351 (1974).

39. The discussion which follows parallels that of F. J. Gilman and M. B. Wise, Phys. Rev. D20, 2392 (1979).

40. M. A. Shifman *et al.*, Zh. Eksp. Teor. Fiz. Pis'ma Red. 22, 123 (1975) [JETP Lett. 22, 55 (1975)]; M. A. Shifman *et al.*, Nucl. Phys. B120, 316 (1977).

41. See F. J. Gilman, SLAC preprint SLAC-PUB-3951, 1986 (to be published in the Proceedings of the Second Aspen Winter Conference).

42. B. Guberina, R. D. Peccei, and R. Ruckl, Phys. Lett. 90B, 169 (1980).

43. For a recent calculation of "penguin" effects in exclusive B decays see M. B. Gavela *et al.*, Phys. Lett. 154B, 425 (1985).

44. H. Krasemann, Phys. Lett. 96B, 397 (1980); E. Golowich, Phys. Lett. 91B, 271 (1980); V. Novikov *et al.*, Phys. Rev. Lett. 38, 626 (1977); I. Bigi and A. Sanda, Phys. Rev. D29, 1393 (1984).

45. B. Grinstein, N. Isgur, and M. B. Wise, Caltech preprint CALT-68-1311, 1986 (unpublished).

46. See, for example, M. L. Goldberger and K. M. Watson, *Collision Theory* (John Wiley, New York, 1964), p.540.

47. H. J. Lipkin, Phys. Rev. Lett. 44, 710 (1980).

48. J. F. Donoghue, Phys. Rev. D33, 1516 (1986).

49. N. Cabibbo and L. Maiani, Phys. Lett. 73B, 418 (1978).

50. M. Bauer and B. Stech, Phys. Lett. 152B, 380 (1985), and M. Bauer, B. Stech, and M Wirbel, Heidelberg University preprint HD-THEP-86-19, 1986 (unpublished); A. J. Buras, J. M. Gerard, and R. Ruckl, Nucl. Phys. B268, 16 (1986).

51. I. Bigi, Refs. 36 and 37.

52. B. Guberina, S. Nussinov, R. D. Peccei, and R. Ruckl, Phys. Lett. 89B, 111 (1979).

53. D. Fakirov and B. Stech, Nucl. Phys. B133, 315 (1978).

54. G. Altarelli and L. Maiani, Phys. Lett. 118B, 414 (1982).

55. M. Bander *et al.*, Phys. Rev. Lett. 44, 7 (1980).

56. W. Bernreuther, O. Nachtmann, and B. Stech, Z. Phys. C4, 257 (1980).

57. H. Fritzsch and P. Minkowski, Phys. Lett. 90B, 455 (1980).